

Role of polarization in probing anomalous gauge interactions of the Higgs boson

Sudhansu S. Biswal¹, Debajyoti Choudhury², Rohini M. Godbole¹ and Mamta³

¹*Centre for High Energy Physics, Indian Institute of Science, Bangalore 560 012, India*

²*Department of Physics and Astrophysics, University of Delhi, Delhi 110 007, India*

³*Department of Physics and Electronics, S.G.T.B. Khalsa College, University of Delhi, Delhi 110 007, India*

Abstract

We explore the use of polarized e^+/e^- beams and/or the information on final state decay lepton polarizations in probing the interaction of the Higgs boson with a pair of vector bosons. A model independent analysis of the process $e^+e^- \rightarrow f\bar{f}H$, where f is any light fermion, is carried out through the construction of observables having identical properties under the discrete symmetry transformations as different individual anomalous interactions. This allows us to probe an individual anomalous term independent of the others. We find that initial state beam polarization can significantly improve the sensitivity to CP -odd couplings of the Z boson with the Higgs boson (ZZH). Moreover, an ability to isolate events with a particular τ helicity, with even 40% efficiency, can improve sensitivities to certain ZZH couplings by as much as a factor of 3. In addition, the contamination from the ZZH vertex contributions present in the measurement of the trilinear Higgs- W (WWH) couplings can be reduced to a great extent by employing polarised beams. The effects of initial state radiation (ISR) and beamstrahlung, which can be relevant for higher values of the beam energy are also included in the analysis.

1 Introduction

Although the Standard Model (SM) has been highly successful in describing all the available experimental data, the precise mechanism of the breaking of the $SU(2) \otimes U(1)$ gauge symmetry and consequent generation of masses for all the elementary particles is still very much an open question. In the SM, the symmetry is broken spontaneously giving rise to masses for all the elementary particles via the Higgs mechanism thereby requiring the presence of a spin-0 CP-even particle, namely the Higgs boson [1–4]. However, so far, there exists no direct experimental evidence for the same. Not surprisingly, therefore, the search for the Higgs boson and the study of its various properties, comprise one of the major aims of all the current and future colliders [5]. The Large Hadron Collider (LHC), soon to go into operation, is expected to shed light on the mechanism of electroweak symmetry breaking (EWSB). It is designed to be capable of finding the SM Higgs boson over most of the theoretically allowed range for its mass [6].

Direct searches at the LEP gives a lower bound on the mass of the SM Higgs boson: $m_H > 114.4$ GeV [7]. On the other hand, electroweak precision measurements put an upper bound

on its mass of about 182 GeV at the 95% confidence level (CL) [8]. Note, though, that these mass bounds are model-dependent and various extensions of the SM admit different allowed ranges of m_H . For example, the lower bound can be relaxed in generic two-Higgs doublet models (2HDM) [9] and more spectacularly in multi-Higgs models with CP violation [10, 11]. As a matter of fact, even in the Minimal Supersymmetric extension of the Standard Model (MSSM) [12], once additional CP-violation is admitted in the scalar sector [10], direct searches at LEP and elsewhere still allow a Higgs boson mass as low as 10 GeV [13]. Similarly, the non-minimal supersymmetric standard model admits very light spin-0 states even without invoking additional sources of CP violation [14]. In certain extensions, the upper bound on the mass of the (lightest) Higgs boson may also be substantially higher [15]. A more detailed discussion of the subject may be found in Refs. [4, 14].

While the SM contains only a single CP-even scalar state, in general, various extensions of the SM mentioned above contain more than one Higgs boson and some, possibly, with different CP properties. For example, the 2HDM—of which the MSSM is a particular case—consists of five spin zero particles: two CP-even neutrals, a CP-odd neutral and a pair of charged scalars. If the MSSM parameters admit CP violation, the neutral particles may no longer be CP eigenstates. The aforementioned dilution of the experimental lower limits is, generically, the result of a reduced coupling of the lightest spin-0 state with the Z due to the mixing of the SM higgs with the other (pseudo)scalars in the model.

Thus, even after the LHC sees a signal for a Higgs boson, a study of its properties (including CP) and precise measurements of its interactions would be necessary to establish the nature of electroweak symmetry breaking. Such a detailed study of this sector may also provide the footprints of new physics beyond the SM. This, though, would be possible only at the International e^+e^- Linear Collider (ILC) [16, 17] and combined information from the ILC and LHC [18, 19], will be required to establish it as *the* SM Higgs boson. A key step in this direction is the determination of the tensor structure of the coupling of the spin-0 state with the different SM particles. A model independent analysis would, then, incorporate the most general form for this tensor structure as allowed by symmetry principles, the anomalous parts having been assumed to have come from effects of high scale physics. The couplings of the Higgs boson with a pair of gauge bosons V ($V = \gamma, W$ and Z) as well as that with a $t\bar{t}$ pair have been studied very thoroughly in the context. The tensor structure can be inferred from kinematical distributions and polarisation measurements for various final state particles. In this study, we concentrate on the trilinear Higgs- Z (ZZH) and Higgs- W (WWH) coupling, in particular focusing on the utility of beam polarisation, measurement of the final state particle polarisation as well as the use of higher beam energies, for the process $e^+e^- \rightarrow f\bar{f}H$.

At an e^+e^- collider, the Z boson produced in the process $e^+e^- \rightarrow ZH$ is, at high energies, longitudinally polarised when produced in association with a CP-even Higgs boson and transversely polarised in case of a CP-odd Higgs boson. The angular and energy distribution of the Z boson can, thus, provide a wealth of information about the ZZH coupling [20, 21]. The shapes of the threshold excitation curve in the processes $e^+e^- \rightarrow ZH$ [22, 23] and $e^+e^- \rightarrow t\bar{t}H$ [24] constitute model independent probes of the tensor structure of the ZZH and the $t\bar{t}H$ coupling respectively. Many detailed studies of how kinematical distributions for the processes $e^+e^- \rightarrow f\bar{f}H$, proceeding via vector boson fusion and Higgs-strahlung can be used to probe the ZZH vertex exist [25, 26]. The anomalous ZZH vertex, in the context of higher dimensional operators has been studied in Refs. [26–35] for a Linear Collider (LC). Ref. [31] is one of the pioneering studies and contains a very extensive analysis, using the optimal observable

technique [36], to probe ZZH and γZH couplings, whereas Refs. [32–34] use asymmetries constructed using differences in the kinematical distributions of the decay products.

The ZZH vertex could be probed at the LHC in a similar fashion, again using kinematic distributions, threshold behaviour as well as asymmetries in the Higgs decays [37–43]. This, alongwith the WWH vertex, can also be studied through vector boson fusion at the LHC [44,45]. Angular distributions of the decay products have been used in Ref. [46] to study the VVH (where $V = Z/W$) vertex in the process $\gamma\gamma \rightarrow H \rightarrow W^+W^-/ZZ$.

In Ref. [34], an exhaustive set of asymmetries, which could probe each of the ZZH anomalous coupling independent of the others, were constructed. Defining kinematical observables which are either odd or even under the different discrete symmetry transformations, the said asymmetries are the expectation values of the sign of these observables. In the approximation of small contribution from anomalous parts (which amounts to retaining terms only upto the linear order in the anomalous couplings), these asymmetries are then proportional to the coefficient of the term in the Lagrangian with the corresponding transformation properties. However, many of these asymmetries turned out to be proportional to the difference between the squared right and left handed couplings of the fermion to the Z boson (viz. $l_f^2 - r_f^2$), and consequently were rather small, on account of the electrons (charged leptons) being involved. It follows then that the sensitivity of these asymmetries to the anomalous couplings could be enhanced by either using the polarized beams or through a measurement of the polarization of the final state particles.

In the unpolarized case, the determination of the anomalous WWH coupling suffers a large contamination from the contribution from the s -channel diagram, arising from the ZZH coupling. We look at the possibility of reducing this contamination by the use of polarised beams. For completely polarized e^+ and e^- beams, σ_{LR} receives contributions from both the Bjorken (s -channel) and fusion (t -channel) diagrams, whereas only the s -channel diagram contributes to σ_{RL} . Thus, beam polarisation may also be used to enhance the sensitivity to WWH anomalous couplings, and this constitutes part of our investigations. Furthermore, we also study the dependence of the sensitivities on the beam energy; again with an aim to enhance the t channel contribution and hence the sensitivity to the WWH couplings. Effects of both initial state radiation (ISR) [47] and beamstrahlung [48,49] have been included in this study as they ought to be.

The rest of the paper is organized as follows: in Sec. 2 we discuss possible sources of anomalous VVH couplings. Various kinematical cuts on final state particles used to suppress the background are discussed in Sec. 3. The ZZH vertex is examined in detail in Sec. 4, with the various observables being defined in Sec. 4.1, the effects of beam polarization being discussed in Sec. 4.2 and the use of final state τ -polarization in Sec. 4.3. In Sec. 4.4 we discuss the improvements possible in the reach for the anomalous ZZH coupling using final state τ measurement with polarised initial beams. In Sec. 5 we construct some observables using the polarisation of initial beams to constrain the WWH couplings. In Sec. 6 we present results on the dependence of the sensitivities to different couplings to the beam energy, including the effects of ISR and beamstrahlung. Finally we summarize our results in Sec. 7.

2 The VVH Couplings

Within the SM/MSSM, the only interaction term involving the Higgs boson and a pair of gauge bosons arises from the Higgs kinetic term in the Lagrangian. However, once we accept the SM to be only an effective low-energy theory, higher-dimensional (and hence non-renormalizable) terms are allowed. The most general VVH vertex, consistent with Lorentz invariance and current conservation¹ can be written as

$$\Gamma_{\mu\nu} = g_V \left[a_V g_{\mu\nu} + \frac{b_V}{m_V^2} (k_{1\nu} k_{2\mu} - g_{\mu\nu} k_1 \cdot k_2) + \frac{\tilde{b}_V}{m_V^2} \epsilon_{\mu\nu\alpha\beta} k_1^\alpha k_2^\beta \right] \quad (1)$$

where k_i denote the momenta of the two W 's (Z 's). Here

$$g_W^{SM} = e \cot \theta_W M_Z, \quad g_Z^{SM} = 2 e M_Z / \sin 2\theta_W,$$

θ_W being the weak-mixing angle and $\epsilon_{\mu\nu\alpha\beta}$ the antisymmetric tensor with $\epsilon_{0123} = 1$. Within the SM, $a_Z = a_W = 1$ and $b_V = \tilde{b}_V = 0$ at tree level. Anomalous parts may arise on account of higher order contributions in a renormalizable theory [50] or from higher dimensional operators in an effective theory [51]. While the imposition of $SU(2)_L \otimes U(1)_Y$ invariance relates the WWH couplings to the ZZH ones, such an assumption restricts the nature of the physics beyond the SM. Instead, we view them purely as phenomenological inputs and study their effect on various final state observables in collider processes.

In general, each of these couplings can be complex, reflecting final state interactions, or equivalently, absorptive parts of the loops either within the SM or from some new physics beyond the SM. However, for each of the observables that we construct for the process $e^+e^- \rightarrow f\bar{f}H$, one overall phase can always be rotated away and we may choose that to be corresponding to either a_Z or a_W . In our analysis, we choose a_Z to be real and allow the others to be complex. Further we also assume a_Z and a_W to be close to there SM value i.e. $a_V = 1 + \Delta a_V$.

For a generic multi-doublet model, supersymmetric or otherwise, couplings of the neutral Higgs bosons to a pair of vector bosons ($V = Z, W$) obey a sum rule [52–54]:

$$\sum_i a_{VH_i}^2 = 1. \quad (2)$$

Although a_{VH_i} for a given Higgs boson in different models, such as MSSM, can be significantly smaller than the SM value, the presence of higher $SU(2)_L$ multiplets or more complicated symmetry breaking structures (such as those within higher-dimensional theories) [54] would lead to more complicated sum rules.

The terms containing a_V and b_V in Eq. 1 constitute the most general coupling of a CP -even Higgs boson with two vector bosons whereas the \tilde{b}_V term corresponds to the CP -odd one. Simultaneous presence of both sets would indicate CP -violation. A non-vanishing value for either $\Im(b_V)$ or $\Im(\tilde{b}_V)$ destroys the hermiticity of the effective theory.

In the context of $SU(2)_L \otimes U(1)_Y$ symmetry, the couplings b_V and \tilde{b}_V can be realized as first order corrections arising from dimension-six operators such as $F_{\mu\nu} F^{\mu\nu} \Phi^\dagger \Phi$ or $F_{\mu\nu} \tilde{F}^{\mu\nu} \Phi^\dagger \Phi$ where Φ is the usual Higgs doublet, $F_{\mu\nu}$ the field strength tensor and $\tilde{F}_{\mu\nu}$ its dual [51]. Of course, higher-order terms may also contribute. Equivalently, the relevant coupling constants may be

¹Terms not respecting current conservation make vanishing contributions once a gauge boson couples to light fermions, as at least one of them must in realistic experimental situations.

thought of as momentum dependent form factors. However, for a theory with a cut-off scale Λ large compared to the energy scale at which the scattering experiment is to be performed, the form-factor behaviour would be very weak and hence can be neglected for our study. Keeping in view the purported higher-order nature of the anomalous couplings, we shall retain only terms up to the linear order in all our expressions.

It is worthwhile to note here that, while our Eq. 1 is the most general expression for the VVH vertex, consistent with Lorentz invariance and current conservation, the process under consideration, namely $e^+e^- \rightarrow Hf\bar{f}$, can, in fact, receive anomalous/non-SM contributions from additional possible operators in an effective theory. Examples include contact interactions such as the dimension-6 $ffVH$ operator [55]

$$\frac{\lambda_{\mathcal{F}}}{\Lambda^2} (\Phi^\dagger D_\mu \Phi) (\bar{\mathcal{F}} \gamma^\mu \mathcal{F})$$

where $\mathcal{F}(\ni f/e)$ denotes a $SU(2)$ multiplet. Even dimension-8 terms such as

$$\frac{g_{ef}}{\Lambda^4} (\Phi^\dagger \Phi) (\bar{e} \gamma^\mu e) (\bar{f} \gamma_\mu f)$$

could contribute. The second term can arise from ultraviolet-complete theories, such as a theory with a Z' and accommodating a $Z'Z'H$ vertex in the limit of a very heavy Z' . The first one, on the other hand, would require a $Z'ZH$ vertex as well. Other constructions, such as theories living in higher dimensions, could also lead to such terms in an appropriate approximation [54]. While the g_{ef} terms can be neglected in an effective theory approach, the $\lambda_{\mathcal{F}}$ terms obviously have to be included in the most general analysis of the process $e^+e^- \rightarrow f\bar{f}H$ [56–58]. Luckily, the contributions of such terms, arising say from a Z' exchange, to the $e^+e^- \rightarrow f\bar{f}H$ amplitude, have the same structure as that due to some of the terms in our anomalous vertex (Eq. 1), as long as $\lambda_{\mathcal{F}}$ are flavour universal. For a generic theory—say, with a Z' whose couplings to fermions are *not* flavour universal—the two contributions may be distinguished from each other by a comparison of possible differences in different channels. In the present work we desist from doing so and thus implicitly assume a flavour universality of the underlying UV-completion (say, the Z' couplings). The only remaining dimension-6 operator that is relevant to the given process is of the form $(\bar{\ell} D_\mu e) (D^\mu \phi)$, where ℓ and e are fermionic $SU(2)$ doublet and singlet respectively. However, owing to a different chirality structure, it does not interfere with the SM amplitude for a massless fermion and hence the corresponding contribution is highly suppressed ($\sim \Lambda^{-4}$).

Various terms in the effective VVH vertex have definite properties under the discrete transformations CP and \tilde{T} , where \tilde{T} stands for the pseudo-time reversal transformation, one which reverses particle momenta and spins but does not interchange initial and final states. Table 1 shows the behaviour under the transformations, CP and \tilde{T} of various operators in the effective Lagrangian, involving different coefficients given in the table.

3 Kinematics and cuts

In this analysis, we largely consider the case of ILC operating at a center of mass energy of 500 GeV and focus on the case of an intermediate mass Higgs boson ($2m_b \leq m_H \leq 140$ GeV), for which $H \rightarrow b\bar{b}$ is the dominant decay mode with a branching fraction $\gtrsim 0.68$ [59]. To be

	a_V	$\Re(b_V)$	$\Im(b_V)$	$\Re(\tilde{b}_V)$	$\Im(\tilde{b}_V)$
CP	+	+	+	-	-
\tilde{T}	+	+	-	-	+

Table 1: Transformation properties of the various operators (identified by their coefficients) in the effective Lagrangian.

specific, we choose the mass of the Higgs boson to be 120 GeV and the b -tagging efficiency to be 0.7.

To be detectable, each of the final state particles in the process $e^+e^- \rightarrow f\bar{f}H(b\bar{b})$, must have a minimum energy and a minimum angular deviation from the beam pipe. Moreover, to be recognized as different entities, they need to be well separated. On the other hand, if the final state contains neutrinos, then the event must be characterized by a minimum missing transverse momentum. Quantitatively, the requirements are

$$\begin{aligned}
E_f &\geq 10 \text{ GeV} && \text{for each visible outgoing fermion} \\
5^\circ \leq \theta_0 &\leq 175^\circ && \text{for each visible outgoing fermion} \\
p_T^{\text{miss}} &\geq 15 \text{ GeV} && \text{for events with } \nu\text{'s} \\
\Delta R_{jj} &\geq 0.7 && \text{for each pair of jets} \\
\Delta R_{\ell\ell} &\geq 0.2 && \text{for each pair of charged leptons} \\
\Delta R_{lj} &\geq 0.4 && \text{for jet-lepton isolation .}
\end{aligned} \tag{3}$$

Here $(\Delta R)^2 \equiv (\Delta\phi)^2 + (\Delta\eta)^2$, $\Delta\phi$ and $\Delta\eta$ being the separation between the two entities in azimuthal angle and rapidity respectively.

In addition, cuts may be imposed on the invariant mass of the $f\bar{f}$ system to enhance(suppress) the contributions coming from s -channel Z -exchange process, namely

$$\begin{aligned}
R1 &\equiv |m_{f\bar{f}} - M_Z| \leq 5\Gamma_Z \implies \text{select } Z\text{-pole ,} \\
R2 &\equiv |m_{f\bar{f}} - M_Z| \geq 5\Gamma_Z \implies \text{de-select } Z\text{-pole ,}
\end{aligned} \tag{4}$$

where Γ_Z is the width of the Z boson. For the $\nu\bar{\nu}H$ final state, the same goal may be reached instead by demanding

$$\begin{aligned}
R1' &\equiv E_H^- \leq E_H \leq E_H^+, \\
R2' &\equiv E_H < E_H^- \text{ or } E_H > E_H^+,
\end{aligned} \tag{5}$$

where $E_H^\pm = (s + m_H^2 - (m_Z \mp 5\Gamma_Z)^2)/(2\sqrt{s})$.

As described earlier, given that the anomalous couplings (\mathcal{B}_i) correspond to operators that are notionally suppressed by some large scale, we need retain terms only upto the linear order. So, any observable \mathcal{O} may be expressed as

$$\mathcal{O}(\{\mathcal{B}_i\}) = \mathcal{O}_{\text{SM}} + \sum O_i \mathcal{B}_i.$$

The possible sensitivity of these observables to \mathcal{B}_i , at a given degree of statistical significance f , can be obtained by demanding that $|\mathcal{O}(\{\mathcal{B}_i\}) - \mathcal{O}_{\text{SM}}| \leq f \Delta\mathcal{O}$. Here $\mathcal{O}(\{0\}) = \mathcal{O}_{\text{SM}}$ is the SM

value of \mathcal{O} and $\Delta\mathcal{O}$ is the fluctuation in the measurement of \mathcal{O} , obtained by adding statistical and systematic errors in quadrature. For example, for \mathcal{O} being the total cross section (σ) or some asymmetry (A), we have

$$\begin{aligned}(\Delta\sigma)^2 &= \sigma/\mathcal{L} + \epsilon^2 \sigma^2, \\(\Delta A)^2 &= \frac{1 - A^2}{\sigma \mathcal{L}} + \frac{\epsilon^2}{2}(1 - A^2)^2.\end{aligned}\tag{6}$$

Here, \mathcal{L} is the integrated luminosity of the e^+e^- collider and ϵ is the fractional systematic error in cross section measurements. Throughout our analysis, we shall take $f = 3$ and $\epsilon = 0.01$. In the approximation of retaining only terms upto linear order in anomalous couplings, the SM values for σ and A are to be used in Eqs. 6.

It may be noted here that in certain cases, such as when

$$\sigma_{\text{SM}} > \frac{1}{\mathcal{L}\epsilon^2}$$

the fluctuations are dominated by the systematic error and thus

$$(\Delta\sigma)^2 \approx \sigma^2 \epsilon^2.$$

For example, the cross sections with the $R2'$ -cut for neutrino final state that are used to constrain WWH couplings in Sec. 5 satisfy this condition and hence the bounds on these couplings are dominated by systematic errors.

4 Anomalous ZZH Couplings

The analysis of Ref. [34] for the case of unpolarised beams had revealed that various asymmetries probing the ZZH anomalous couplings were in fact proportional to $(l_f^2 - r_f^2)$ where l_f (r_f) denote the coupling of a Z boson to a left-(right-)handed fermion. Use of polarised beams or detection of a τ with a specific polarisation in the final state can then avoid the cancellation between these two terms and may lead to an enhancement in sensitivity. In this section, we analyse various observables that can be constructed with the use of these two quantities.

4.1 Observables

Starting from various kinematical quantities C_i constructed as various combinations of the different particle momenta and their spins, we define observables \mathcal{O}_i , as expectation values of the signs of C_i , i.e. $\mathcal{O}_i = \langle \text{sign}(C_i) \rangle$ (C_i 's, $i \neq 1$). Each of these observables transform in a well-defined manner under C , P and \tilde{T} , and within the aforementioned linear approximation, may be used to probe the contribution of a given operator(s) in the effective Lagrangian with the same transformation properties². In fact, the observables listed here are the same ones as considered in Ref. [34], but here we use them for a specific polarisation of initial beams and final state τ 's. Needless to say, we concentrate on the cases where use of polarisation affords a distinct gain in sensitivity. Table 2 lists some of these observables (cross sections and various asymmetries), their transformation properties and the anomalous coupling they may constrain; and, below, we give a description of the same:

²Henceforth, we shall interchangeably use the terminology “transformation properties of anomalous couplings” for those of the corresponding operator in the effective Lagrangian.

ID	\mathcal{C}_i	C	P	CP	\tilde{T}	$CPT\tilde{T}$	Observable(\mathcal{O}_i)	Coupling
1	1	+	+	+	+	+	σ	$a_z, \Re(b_z)$
2	$\vec{P}_e \cdot \vec{p}_H$	-	+	-	+	-	A_{FB}	$\Im(\tilde{b}_z)$
3	$(\vec{P}_e \times \vec{p}_H) \cdot \vec{P}_f$	+	-	-	-	+	A_{UD}	$\Re(\tilde{b}_z)$
4	$[\vec{P}_e \cdot \vec{p}_H] * [(\vec{P}_e \times \vec{p}_H) \cdot \vec{P}_f]$	-	-	+	-	-	A_{comb}	$\Im(b_z)$
5	$[\vec{P}_e \cdot \vec{p}_f] * [(\vec{P}_e \times \vec{p}_H) \cdot \vec{P}_f]$	\otimes	-	\otimes	-	\otimes	A'_{comb}	$\Im(b_z), \Re(\tilde{b}_z)$

Table 2: Various possible \mathcal{C}_i 's, their transformation properties, the associated observables \mathcal{O}_i and the anomalous couplings on which they provide information. The symbol \otimes indicates the lack of a definitive transformation property. Here, $\vec{P}_e \equiv \vec{p}_{e^-} - \vec{p}_{e^+}$, $\vec{P}_f \equiv \vec{p}_f - \vec{p}_{\bar{f}}$ and \vec{p}_H is the momentum of Higgs boson (to be deduced from the measurement of its decay products).

- \mathcal{O}_1 is nothing but the total cross section as obtained with a specific choice of polarisation for the initial beams and/or that for a final state τ . As we retain contributions only upto the lowest non-trivial order in the anomalous couplings (keeping in view the higher dimensional nature of their origin), the differential cross section can be expressed as

$$d\sigma = \sum_{V=Z,W} [(1 + 2 \Re(\Delta a_V)) d\sigma_{0V} + \Im(\Delta a_V) d\sigma'_{0V} + \Re(b_V) d\sigma_{1V} + \Re(\tilde{b}_V) d\sigma_{2V} + \Im(b_V) d\sigma_{3V} + \Im(\tilde{b}_V) d\sigma_{4V}]. \quad (7)$$

where, as in Ref. [34], we have assumed that the Higgs is SM-like and hence

$$a_V \equiv 1 + \Delta a_V \quad (8)$$

is close to its SM value. As stated before we choose a_Z to be real, hence $\Im(\Delta a_Z) = 0$ and we denote $\Re(\Delta a_Z) = \Delta a_Z$.

- \mathcal{O}_2 is simply the forward-backward(FB) asymmetry with respect to polar angle of the Higgs boson, namely

$$A_{\text{FB}}(\cos \theta_H) = \frac{\sigma(\cos \theta_H > 0) - \sigma(\cos \theta_H < 0)}{\sigma(\cos \theta_H > 0) + \sigma(\cos \theta_H < 0)} \quad (9)$$

Since $\mathcal{C}_2 \equiv \vec{P}_e \cdot \vec{p}_H$ is odd under CP and even under \tilde{T} transformation, this observable would thus be proportional to $\Im(\tilde{b}_z)$.

- \mathcal{O}_3 is the up-down(UD) asymmetry defined in terms of the momentum of the final state fermion f with respect to the H -production plane:

$$A_{\text{UD}} = \frac{\sigma(\sin \phi > 0) - \sigma(\sin \phi < 0)}{\sigma(\sin \phi > 0) + \sigma(\sin \phi < 0)}. \quad (10)$$

As $\mathcal{C}_3 \equiv (\vec{P}_e \times \vec{p}_H) \cdot \vec{P}_f$ is odd under both CP and \tilde{T} , one may use this to probe $\Re(\tilde{b}_z)$.

4. $\mathcal{C}_4 \equiv [\vec{P}_e \cdot \vec{p}_H] * [(\vec{P}_e \times \vec{p}_H) \cdot \vec{P}_f]$ is even under CP and odd under \tilde{T} and thus expected to be sensitive to $\Im(b_Z)$. The corresponding observable \mathcal{O}_4 is a particular combination of the polar and azimuthal asymmetries (designed to increase sensitivity) and is defined as

$$A_{comb} = \frac{\sigma_{FU} + \sigma_{BD} - \sigma_{FD} - \sigma_{BU}}{\sigma_{FU} + \sigma_{BD} + \sigma_{FD} + \sigma_{BU}}, \quad (11)$$

where F, B, U and D refer to the restricted phase space as mentioned above in \mathcal{O}_2 and \mathcal{O}_3 . Thus σ_{FU} refers to the cross section with Higgs boson restricted to be produced in forward hemi-sphere with respect to the initial state electron and the final state fermion is produced above the H -production plane.

5. \mathcal{O}_5 is yet another asymmetry derived from a combination of polar and azimuthal distributions and is given by:

$$A'_{comb} = \frac{\sigma_{F'U} + \sigma_{B'D} - \sigma_{F'D} - \sigma_{B'U}}{\sigma_{F'U} + \sigma_{B'D} + \sigma_{F'D} + \sigma_{B'U}}. \quad (12)$$

Here F' (B') refer to the production of f in forward (backward) hemi-sphere with respect to the initial state e^- , whereas U and D are the same as defined before. This being both P - and \tilde{T} -odd and with no specific C transformation, can be used to probe both $\Im(b_Z)$ and $\Re(\tilde{b}_Z)$.

Note that the asymmetries \mathcal{O}_3 , \mathcal{O}_4 and \mathcal{O}_5 require charge measurement of the final state particles and hence events with light quarks in the final state can not be considered for these observables.

4.2 Effect of Beam Polarization

For longitudinally polarized beams, the cross section can be written as

$$\begin{aligned} \sigma(\mathcal{P}_{e^-}, \mathcal{P}_{e^+}) &= \frac{1}{4} \left[(1 + \mathcal{P}_{e^-})(1 + \mathcal{P}_{e^+})\sigma_{RR} + (1 + \mathcal{P}_{e^-})(1 - \mathcal{P}_{e^+})\sigma_{RL} \right] \\ &+ \frac{1}{4} \left[(1 - \mathcal{P}_{e^-})(1 + \mathcal{P}_{e^+})\sigma_{LR} + (1 - \mathcal{P}_{e^-})(1 - \mathcal{P}_{e^+})\sigma_{LL} \right], \end{aligned}$$

where σ_{LR} corresponds to the case of the electron (positron) beams being completely left(right) polarized respectively, i.e. , $\mathcal{P}_{e^-} = -1$, $\mathcal{P}_{e^+} = +1$. σ_{RR} , σ_{RL} and σ_{LL} are defined analogously. While the ideal case of complete polarisation is impossible to achieve, values of 80%(60%) polarisation for e^- (e^+) seem possible at the ILC [17]. Taking these to be our default values, we denote:

$$\sigma^{-,+} = \sigma(\mathcal{P}_{e^-} = -0.8, \mathcal{P}_{e^+} = 0.6) \quad (13)$$

and similarly for other combinations, viz. $\sigma^{+,+}$, $\sigma^{+,-}$ and $\sigma^{-,-}$. We concentrate here on the observables discussed in the Sec. 4.1 for specific polarization combinations. We would find that polarization plays a crucial role in probing the CP-odd ZZH couplings, while the improvement in sensitivity in the others is only marginal.

We quote all our results for an integrated luminosity of 500 fb^{-1} and a degree of statistical significance $f = 3$ assuming the fractional systematic error to be 1% i.e. ϵ of Eq. 6 to be 0.01. Denoting the four possible polarization combinations by

$$\begin{aligned} a &: (-, +), & b &: (+, -), \\ c &: (-, -), & d &: (+, +), \end{aligned} \quad (14)$$

we consider two possible ways of dividing the luminosity amongst these runs, namely

$$\begin{aligned} \text{option (i) : } \quad \mathcal{L} &= 125 \text{ fb}^{-1} && \text{for each of } (a, b, c, d) \\ \text{option (ii) : } \quad \mathcal{L} &= \begin{cases} 200 \text{ fb}^{-1} & \text{for } (a, b) \\ 50 \text{ fb}^{-1} & \text{for } (c, d) \end{cases} \end{aligned} \quad (15)$$

While option (i) is a straightforward choice, option (ii) is better appreciated on realizing that polarization combinations (c, d) suppress both SM s -channel processes as also WW -fusion. Thus, although these combinations maybe useful for certain physics beyond the SM, it is not certain whether such modes would find favour for generic search strategies.

4.2.1 Δa_Z and $\Re(b_Z)$

It is obvious that the contribution of Δa_Z would be identical in form to that within the SM and, thus, such a coupling can be probed only through a deviation of the cross sections from the SM expectations. As for $\Re(b_Z)$, the fact that this term too conserves each of C , P and \tilde{T} , renders all asymmetries insensitive to it. Thus, this coupling too needs to be measured from cross sections alone.

Clearly, just one measurement cannot resolve between these two couplings, and this problem was faced by the analysis of Ref. [34] as well. Presumably, with beam polarization being available, cross section measurement for a variety of polarization states would offer additional information. However, as far as the Bjorken process goes, this dependence is, understandably, trivial and identical for both of Δa_Z and $\Re(b_Z)$. This is attested to by the first two rows of Table 3, which in fact lists different anomalous contributions to cross sections corresponding to different initial state polarisation combinations and different final states. For $e^+e^- \rightarrow e^+e^-H$ though, two diagrams contribute, the usual s -channel one and an additional t -channel one (ZZ fusion), with the polarization dependence of the latter being grossly different. To accentuate this, we may de-select the Z -pole (the $R2$ -cut of Eq. 4) and the corresponding cross sections are displayed in Table 3. For completely polarized e^\pm beams, LR and RL are the CP -eigen states, whereas LL and RR states are CP -conjugate to each other. Hence σ_{LL} and σ_{RR} receive additional contribution from $\Im(\tilde{b}_Z)$ and this is reflected in Table 3. In addition, this contribution is proportional to $(\mathcal{P}_{e^-} + \mathcal{P}_{e^+})$ and thus would vanish if the average values of this quantity vanishes (as, for example, happens in the unpolarized case). More importantly, the $\Re(b_Z)$ contribution to the ZZ -fusion diagram has an opposite dependence on the product $(\mathcal{P}_{e^-}\mathcal{P}_{e^+})$ as compared to that of the a_Z piece. This may be exploited to construct an appropriate observable, namely

$$\begin{aligned} \mathcal{O}_A &= 1.3(\mathcal{O}'_{1a} + \mathcal{O}'_{1b}) + (\mathcal{O}'_{1c} + \mathcal{O}'_{1d}) \\ &= [15.1(1 + 2\Delta a_z) + 0.038 \Re(b_Z)] \text{ fb} \end{aligned} \quad (16)$$

That the contribution of $\Im(\tilde{b}_Z)$ in Eq. 16 vanishes identically is easy to understand. Even though the relative weights of the two terms in Eq. 16 can be tuned to reduce the coefficient of $\Re(b_Z)$ further, it is not really necessary, since both Δa_Z and $\Re(b_Z)$ are expected to arise, say at one-loop, and hence would have similar order of magnitude. The large difference in the relative weights renders $\Re(b_Z)$ almost irrelevant, making it plausible to constrain Δa_z independent of $\Re(b_Z)$. A lack of deviation of \mathcal{O}_A from its SM value would give a 3σ level limit on Δa_z of the form

$$|\Delta a_Z| \leq \begin{cases} 0.038 & \text{for option (i)} \\ 0.043 & \text{for option (ii)}. \end{cases} \quad (17)$$

Observable	Description	σ_{0Z}	σ_{1Z}	σ_{4Z}
\mathcal{O}_{1a}	$\sigma^{-,+}(R1; \mu, q)$	23.9	226	0
\mathcal{O}_{1b}	$\sigma^{+,-}(R1; \mu, q)$	17.9	169	0
\mathcal{O}'_{1a}	$\sigma^{-,+}(R2; e)$	4.04	1.46	0.122
\mathcal{O}'_{1b}	$\sigma^{+,-}(R2; e)$	2.64	0.715	-0.122
\mathcal{O}'_{1c}	$\sigma^{-,-}(R2; e)$	3.29	-1.34	0.855
\mathcal{O}'_{1d}	$\sigma^{+,+}(R2; e)$	3.09	-1.45	-0.855

Table 3: Various anomalous contributions (as defined in Eq. 7) to the cross sections $\sigma(R1; \mu, q)$ (for μ^\pm and light quarks in the final state with R1-cut) and $\sigma(R2; e)$ (for e^\pm in the final state with R2-cut) for the four polarisation states. The rates are in femtobarns, for $\sqrt{s} = 500$ GeV.

The smallness of the difference in the two limits is but a consequence of the larger error bars resulting from smaller luminosities assigned to polarization combinations (c, d). Note that the limits are only marginally different from that obtained with unpolarised beams with $\mathcal{L} = 500 \text{ fb}^{-1}$, namely of $|\Delta a_Z| \lesssim 0.04$ [34]³. More importantly, though, unlike the bound of Ref. [34], the constraint of Eq. 17 is independent of $\Re(b_Z)$.

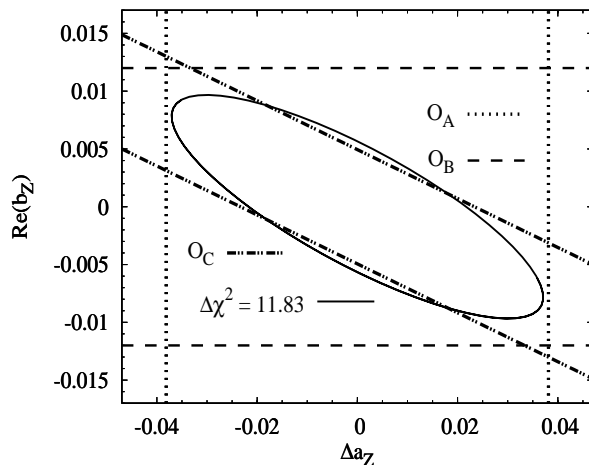


Figure 1: The regions in the $\Delta a_Z - \Re(b_Z)$ plane consistent with 3σ variations in the observables $\mathcal{O}_{A,B,C}$ respectively. The region enclosed by all the three sets reflect the overall constraints. The ellipse represents the region corresponding to $\Delta\chi^2 = 11.83$ obtained using all polarised cross sections listed in Table 3. An integrated luminosity of 125 fb^{-1} for each of the polarisation state i.e. option (i) of Eq. 15 has been used. The limits for option (ii) are very similar.

A different linear combination of the same observables, namely,

$$\begin{aligned}
\mathcal{O}_B &= \mathcal{O}_{1a} + \mathcal{O}_{1b} - 6.6(\mathcal{O}'_{1c} + \mathcal{O}'_{1d}) \\
&= [-0.31(1 + 2\Delta a_Z) + 413\Re(b_Z)] \text{ fb}
\end{aligned}
\tag{18}$$

³Note that the results quoted here for the unpolarised beams differ from those of the Ref. [34] because of the difference in the value of branching fraction of $H \rightarrow b\bar{b}$ decay mode used there. We have used the value of branching fraction to be 0.68 whereas in Ref. [34] it was taken to be 0.9

is equally useful as this enhances the $\Re(b_Z)$ contribution, while essentially getting rid of Δa_Z . This leads to

$$|\Re(b_Z)| \leq \begin{cases} 0.012 & \text{for option (i)} \\ 0.018 & \text{for option (ii)} \end{cases} \quad (19)$$

virtually independent of Δa_Z . Finally, using the information from the $R1$ -cut alone, we have

$$\begin{aligned} \mathcal{O}_C &= \mathcal{O}_{1a} + \mathcal{O}_{1b} \\ &= [41.8(1 + 2\Delta a_Z) + 395 \Re(b_Z)] \text{ fb} \end{aligned} \quad (20)$$

leading to a correlated constraint in the Δa_Z - $\Re(b_Z)$ plane as displayed in Fig. 1. Of the six cross sections of Table 3, one may be used to eliminate $\Im(\tilde{b}_Z)$, leaving behind five constraints in this plane. Note that we have already used three linearly independent combinations. We may, nonetheless, use all five to construct a χ^2 -test. The resultant 3σ ellipse (corresponding to $\Delta\chi^2 = 11.83$) is also displayed in Fig. 1. That this ellipse protrudes slightly beyond the set of straight lines is not surprising, for the latter denote the 3σ constraint on a particular combination of the two variables (with complete disregard for the orthogonal combination), while the ellipse gives the corresponding bound on the plane. Furthermore, the size and the shape of the ellipse demonstrates that the three combinations identified above represent the strongest constraints with very little role played by the remaining two.

Finally, recollect that, for completely polarized e^\pm beams, LL and RR states are CP -conjugate to each other. Hence the difference of σ_{LL} and σ_{RR} can be used to probe CP -odd couplings. Thus, using

$$\mathcal{O}_D \equiv \mathcal{O}'_{1c} - \mathcal{O}'_{1d} = [0.2(1 + 2\Delta a_Z) + 0.11 \Re(b_Z) + 1.71 \Im(\tilde{b}_Z)] \text{ fb} , \quad (21)$$

one obtains

$$|\Im(\tilde{b}_Z)| \leq 0.4 \quad \text{for } \mathcal{L} = 125 \text{ fb}^{-1}. \quad (22)$$

However, a better constraint can be obtained on this coupling with the use of FB-asymmetry with respect to polar angle of Higgs boson and a discussion of this follows.

4.2.2 $\Re(\tilde{b}_Z)$ and $\Im(\tilde{b}_Z)$

Next we focus on the role of beam polarisation in exploring both the real and imaginary parts of \tilde{b}_Z . As discussed earlier, the independent experimental probes for these couplings, namely the asymmetries A_{FB} and A_{UD} , are proportional to the quantity $(l_e^2 - r_e^2)$ for the case of unpolarised beams [34]. For maximally polarized beams, on the other hand, the squared matrix element is either proportional to r_e^2 or to l_e^2 and hence the suppression factor is not so severe even for moderate polarization. Since $l_e^2 > r_e^2$, the cross sections are somewhat larger for the polarization combination $a \equiv (-, +)$, and hence the corresponding constraints would turn out to be a little stronger.

Imposing the various kinematical cuts of Eq. 3, along-with the $R1$ -cut of Eq. 4 to select Z -pole contribution, the forward-backward (referring to the Higgs polar angle) asymmetry for different final states and with different polarisation states of the initial beams, can be written,

keeping terms up to linear order in anomalous couplings, as

$$A_{FB}^{-,+}(R1 - \text{cut}) = \begin{cases} \frac{0.174 \Re(\tilde{b}_Z) - 6.14 \Im(\tilde{b}_Z)}{1.48} & (e^+e^-H) \\ \frac{-6.07 \Im(\tilde{b}_Z)}{1.46} & (\mu^+\mu^-H) \\ \frac{-92.8 \Im(\tilde{b}_Z)}{22.4} & (q\bar{q}H) \end{cases} \quad (23)$$

and

$$A_{FB}^{+,-}(R1 - \text{cut}) = \begin{cases} \frac{-0.0911 \Re(\tilde{b}_Z) + 4.43 \Im(\tilde{b}_Z)}{1.11} & (e^+e^-H) \\ \frac{4.4 \Im(\tilde{b}_Z)}{1.09} & (\mu^+\mu^-H) \\ \frac{67.2 \Im(\tilde{b}_Z)}{16.8} & (q\bar{q}H) \end{cases} \quad (24)$$

Here, each of the numerical factors denote cross-sections in femtobarns with the denominator being the SM cross section. Understandably, the FB asymmetry is identical for the case of the Z going into muons or a $q\bar{q}$ pair, and thus the two channels can be added up to obtain the total sensitivity. As for the e^+e^-H channel, the coupling $\Re(\tilde{b}_Z)$ makes an appearance on account of the interference of the t -channel diagram with the absorptive part of the s -channel SM one.

The FB-asymmetry with final state μ 's and q 's get contribution only from $\Im(\tilde{b}_Z)$. Hence we define the following observable

$$\begin{aligned} \mathcal{O}_{FB}(R1; \mu, q) &= A_{FB}^{-,+}(R1; \mu) + A_{FB}^{-,+}(R1; q) - A_{FB}^{+,-}(R1; \mu) - A_{FB}^{+,-}(R1; q) \\ &= -16.3 \Im(\tilde{b}_Z) \end{aligned} \quad (25)$$

which leads to

$$|\Im(\tilde{b}_Z)| \leq \begin{cases} 0.011 & \text{for option (i)} \\ 0.0089 & \text{for option (ii)}. \end{cases} \quad (26)$$

In Fig. 2, the vertical lines represent the above bounds for option (i).

Similarly, the up-down asymmetries, with respect to azimuthal angle of final state fermions, are given by

$$A_{UD}^{-,+}(R1 - \text{cut}) = \begin{cases} \frac{-1.43 \Re(\tilde{b}_Z) - 0.286 \Im(\tilde{b}_Z)}{1.48} & (e^+e^-H) \\ \frac{-1.49 \Re(\tilde{b}_Z)}{1.46} & (\mu^+\mu^-H) \end{cases} \quad (27)$$

and

$$A_{UD}^{+,-}(R1 - \text{cut}) = \begin{cases} \frac{1.12 \Re(\tilde{b}_Z) - 0.161 \Im(\tilde{b}_Z)}{1.11} & (e^+e^-H) \\ \frac{1.08 \Re(\tilde{b}_Z)}{1.09} & (\mu^+\mu^-H) \end{cases} \quad (28)$$

Since the determination of this asymmetry requires charge measurement of the final state particles, we do not consider it for quarks in the final states. Once again, $\Im(\tilde{b}_Z)$ makes an

appearance for the e^+e^-H case on account of the aforementioned interference. Combining both polarisation states $(-, +)$ and $(+, -)$ for final state muons we construct a observable, namely,

$$\mathcal{O}_{UD}(R1; \mu) \equiv A_{UD}^{-,+}(R1; \mu) - A_{UD}^{+,-}(R1; \mu) = -2.01 \Re(\tilde{b}_Z), \quad (29)$$

we may constrain

$$|\Re(\tilde{b}_Z)| \leq \begin{cases} 0.17 & \text{for option (i)} \\ 0.13 & \text{for option (ii)}. \end{cases} \quad (30)$$

Clearly, one expects a nontrivial effect of the beam polarisation only for asymmetries constructed with the $R1$ -cut. For the sake of completeness, we also present the up-down asymmetries with the $R2$ -cut (de-selecting the Z -pole) for the eeH final state, namely

$$\begin{aligned} A_{UD}^{-,+}(R2; e) &= \frac{4.3 \Re(\tilde{b}_Z) + 0.227 \Im(b_Z)}{4.04}, \\ A_{UD}^{+,-}(R2; e) &= \frac{3 \Re(\tilde{b}_Z) - 0.227 \Im(b_Z)}{2.64}, \\ A_{UD}^{-,-}(R2; e) &= \frac{4.01 \Re(\tilde{b}_Z) + 1.59 \Im(b_Z)}{3.29}, \\ A_{UD}^{+,+}(R2; e) &= \frac{3.82 \Re(\tilde{b}_Z) - 1.59 \Im(b_Z)}{3.09}. \end{aligned} \quad (31)$$

With LL and RR initial states being CP -conjugate to each other, it is understandable that A_{UD} receives additional contribution⁴ from $\Im(b_Z)$. Defining

$$\begin{aligned} \mathcal{O}_{UD}(R2; e) &= 2 A_{UD}^{-,+}(R2; e) + A_{UD}^{+,-}(R2; e) + A_{UD}^{-,-}(R2; e) + A_{UD}^{+,+}(R2; e) \\ &= 5.72 \Re(\tilde{b}_Z) - 0.005 \Im(b_Z) \end{aligned} \quad (32)$$

one may get rid of this contribution, and thereby constrain

$$|\Re(\tilde{b}_Z)| \leq \begin{cases} 0.067 & \text{for option (i)} \\ 0.074 & \text{for option (ii)} \end{cases} \quad (33)$$

at the 3σ level. The bounds for option (i) are represented by horizontal lines in Fig. 2.

It is instructive to compare the above sensitivities (see Table 4) with those possible with unpolarised beams [34]. As one can see, for asymmetries with $R1$ -cut, the enhancement of sensitivity to both the CP -odd couplings $\Re(\tilde{b}_Z)$ and $\Im(\tilde{b}_Z)$ on using longitudinally polarized beams for option (ii)(option (i)) of Eqs. 15) is nearly by a factor of 7(5–6), a feat unachievable without polarisation. This improvement is indeed due to the circumvention of the vanishingly small vector coupling of electron to the Z boson. Our results are compatible with the more stringent limits of Ref. [33], when we remove the effect of kinematical cuts as well as of the use of the $b\bar{b}$ final state and finite b -tagging efficiency, implemented in our analysis. Of course, a similar enhancement for $\Re(\tilde{b}_Z)$ may also be possible even with unpolarised beams, when A_{UD} for the eeH final state is considered alongwith the $R2$ -cut. It is, nonetheless, interesting to have two different measurements measure the same coupling to the same accuracy. Of course, this in addition to the big enhancement in sensitivity to the CP -odd couplings $\Re(\tilde{b}_Z)$ and $\Im(\tilde{b}_Z)$ as mentioned above; this, in fact, is not achievable with the $R1$ -cut.

⁴This is analogous to the appearance of $\Im(\tilde{b}_Z)$ in the total cross sections in Sec.4.2.1.

Using Polarized Beams				Unpolarized States	
Coupling	Limits		Observable used	Limits	Observable used
	Option(i)	Option(ii)			
$ \Re(\tilde{b}_Z) \leq$	0.067	0.074	$\mathcal{O}_{UD}(R2; e)$	0.067	$A_{UD}(R2; e)$
$ \Re(\tilde{b}_Z) \leq$	0.17	0.13	$\mathcal{O}_{UD}(R1; \mu)$	0.91	$A_{UD}(R1; \mu)$
$ \Im(\tilde{b}_Z) \leq$	0.011	0.0089	$\mathcal{O}_{FB}(R1; \mu, q)$	0.064	$A_{FB}(R1; \mu, q)$

Table 4: Limits on anomalous ZZH couplings from various observables at 3σ level for both polarized and unpolarized beams. While an integrated luminosity of 500 fb^{-1} is assumed for the unpolarized run, for the polarized case the same is divided according to the options of Eq. 15.

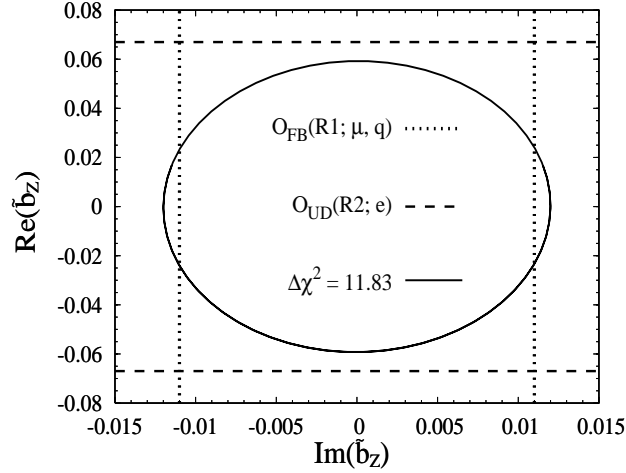


Figure 2: The regions in the $\Im(\tilde{b}_Z)$ - $\Re(\tilde{b}_Z)$ plane consistent with 3σ variations in the observables $\mathcal{O}_{FB}(R1; \mu, q)$ and $\mathcal{O}_{UD}(R2; e)$. The vertical and horizontal lines are for respective variation in them. The ellipse represents the region corresponding to a 3σ bound in the plane ($\Delta\chi^2 = 11.83$) obtained using all asymmetries listed in Eqs. 23, 24, 27, 28, 31. Option (i) of luminosity division has been assumed.

A further improvement is possible if all the asymmetries listed in Eqs. (23,24, 27,28) are considered alongwith the three independent combinations obtained from Eqs. 31 by eliminating $\Im(b_Z)$ therefrom. Once again, a χ^2 can be constructed leading to a 3σ contour as displayed in Fig. 2.

And, finally, we use the remaining information available from Eqs. 31 to probe $\Im(b_Z)$. Defining

$$\mathcal{O}'_{UD}(R2; e) \equiv A_{UD}^{-,-}(R2; e) - A_{UD}^{+,+}(R2; e) = -0.017 \Re(\tilde{b}_Z) + 0.998 \Im(b_Z), \quad (34)$$

we may impose

$$|\Im(b_Z)| \leq 0.22 \quad \text{for } \mathcal{L} = 125 \text{ fb}^{-1}. \quad (35)$$

This limit is only marginally different than the one obtained with unpolarised beams using the combined asymmetry A_{comb} of Sec. 4.1 with $R1$ -cut. We shall see in the next section that a better constraint may be obtained on this coupling from the combined asymmetry if the final state τ helicity is measured.

4.3 Use of Final State τ Polarization with Unpolarised Beams.

In this section we report on the use of selecting final states with τ 's in a given helicity state. A similar idea was employed in the optimal variable analysis of Ref. [31]. A detailed measurement of the decay pion energy distribution [60] or a simpler measurement of the inclusive single pion spectrum [61], can yield information on τ polarisation. Discussions exist in literature on how this can be utilized to sharpen search strategies for charged Higgs boson [60–66] or supersymmetric partners [67] and even for the measurement of SUSY parameters [68, 69]. In a similar vein, one can also construct observables using the final state τ polarisation to probe ZZH couplings. We construct asymmetries for τ with definite polarisation which can be measured in simple counting experiments and which can catch the essence of the above mentioned optimal observable analysis.

As discussed in Ref. [34], for unpolarized initial and final states, the combined polar-azimuthal asymmetry A_{comb} is proportional to $(\ell_e^2 + r_e^2)(r_f^2 - \ell_f^2)$ and the up-down asymmetry, $A_{UD}(\phi)$ is proportional to $(\ell_e^2 - r_e^2)(r_f^2 - \ell_f^2)$. Thus, for leptonic final states, both these asymmetries suffer a suppression (this is particularly important for both A_{UD} and A_{comb} which are impossible to measure with hadronic final states). Hence, the measurement of the final state τ polarisation would lead to an enhancement in these symmetries with a consequent improvement in the sensitivity to both of the \tilde{T} -odd anomalous couplings, namely $\Im(b_Z)$ and $\Re(\tilde{b}_Z)$. Further, since $\ell_\tau^2 > r_\tau^2$, one gets a slightly higher gain in sensitivity with final state τ in a negative helicity state.

To demonstrate this, we construct various asymmetries (listed in Table 2) for both left- and right-handed τ in the final state. These are the same as described in Sec. 4.1 but defined for a particular helicity of τ rather than for a specific initial beam polarisation state (for this analysis we take the initial state to be unpolarised). Again, after imposing the kinematical cuts of Eq. 3

alongwith the $R1$ -cut, these read

$$\begin{aligned}
A_{UD}^L(R1; \tau) &= \frac{-0.527 \Re(\tilde{b}_Z)}{0.495}, \\
A_{UD}^R(R1; \tau) &= \frac{0.388 \Re(\tilde{b}_Z)}{0.365}, \\
A_{\text{comb}}^L(R1; \tau) &= \frac{-1.37 \Im(b_Z)}{0.495}, \\
A_{\text{comb}}^R(R1; \tau) &= \frac{1.01 \Im(b_Z)}{0.365}, \\
A'_{\text{comb}}^L(R1; \tau) &= \frac{1.18 \Im(b_Z) - 0.3 \Re(\tilde{b}_Z)}{0.495}, \\
A'_{\text{comb}}^R(R1; \tau) &= \frac{-0.868 \Im(b_Z) - 0.221 \Re(\tilde{b}_Z)}{0.365}.
\end{aligned} \tag{36}$$

where the numbers represent the partial (total) cross sections in femtobarns. As expected, the asymmetries are, generically, in the opposite sense for left- and right-handed τ 's (and, hence, would have largely cancelled each other). Thus, being able to isolate τ 's of a given helicity indeed can add to the sensitivity and the slightly larger value of l_τ means that the final state with negative helicity τ 's will be even better. Rather than effect a detailed analysis, we make a simplifying and *illustrative* assumption that final state τ^- 's in a specific (negative or positive) helicity state can be isolated with very high purity at the cost of an efficiency of 40% or even 20%. Under this assumption, we list, in Table 5, the best limits that are possible for the \tilde{T} -odd couplings $\Im(b_z)$ and $\Re(\tilde{b}_Z)$ using asymmetries of Eq. 36 for negative helicity τ 's. (The positive helicity τ 's would lead to very similar (marginally weaker) bounds, and we omit these for ease of presentation.) Corresponding limits obtainable with the τ final state but without using knowledge of τ helicity are also shown for comparison.

Coupling	Using Pol. of final state τ^-			Unpolarised τ 's	
	Limits		Observable	Limits	Observable
	40% eff.	20% eff.			
$ \Im(b_z) \leq$	0.11	0.15	A_{comb}^L	0.35	A_{comb}
$ \Re(\tilde{b}_Z) \leq$	0.28	0.40	A_{UD}^L	0.91	A_{UD}

Table 5: *Limits on anomalous ZZH couplings from various observables at 3σ level with negatively polarised and unpolarised τ 's (i.e. without using knowledge of τ helicity), with R1-cut.*

It is clear from Table 5 that the limits on $\Im(b_Z)$ and $\Re(\tilde{b}_Z)$ can be improved by the measurement of the final state τ polarization. Preliminary results of our analysis were presented in Ref. [70]. A similar observation had been made earlier in the context of optimal observable analysis [31]. It is to be noted here that the unpolarized measurements with eeH final state, with $R2$ -cut gives a better sensitivity to $\Re(\tilde{b}_Z)$ as discussed earlier. It is, however, nice to have more than one observable determining a given coupling. We would like to stress here that even with an efficiency of isolating events with a given τ^- helicity as low as 20%, this method affords an increase in the sensitivity for $\Im(b_Z)$ by as much as a factor ~ 2 .

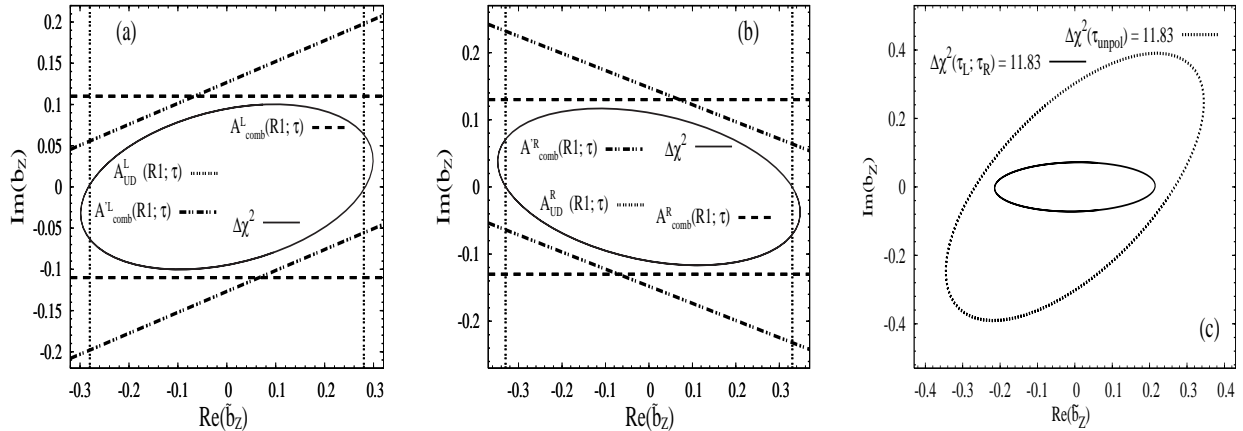


Figure 3: 3σ blind regions in the $\Re(\tilde{b}_Z) - \Im(b_Z)$ for a τ -helicity isolation efficiency of 40% and an integrated luminosity of 500 fb^{-1} . Panel **a** (**b**) is for left-(right-)handed τ^- 's. The horizontal, vertical and oblique lines correspond to A_{comb} , A_{UD} and A'_{comb} respectively. The ellipse combines all three and represents the blind region in the plane. The inner ellipse of panel (**c**) combines both sets, and the outer represents the constraints without using τ -helicity information.

Fig. 3 displays the region in $\Re(\tilde{b}_Z) - \Im(b_Z)$ plane that can be probed using the asymmetries of Eq. 36 for τ^- 's in a specific helicity state, for an isolation efficiency of 40%. Once again, a χ^2 test can be constructed trivially. Note that the constraint from A'_{comb} are in opposite sense for left- and right-handed τ^- 's, resulting in a rotation of the two 3σ ellipses with respect to each other. One may then combine the information obtained from the two final states and the results thereof are shown in the last panel. The fact of the two individual ellipses being only slightly rotated with respect to the $\Re(\tilde{b}_Z)$ axes means that this exercise of combining the two leads to only a moderate improvement. It is interesting, though, to compare the result with the corresponding region when the τ -helicity information is unavailable. The difference is obvious.

4.4 Use of final state τ polarisation for polarised beams

Having established that each of beam polarization and measurement of τ -helicity can lead to substantial improvements, the natural question relates to the combination of the two effects. Recall that the up-down asymmetry A_{UD} is proportional to $(l_e^2 - r_e^2)(l_\tau^2 - r_\tau^2)$ while the combined asymmetry A_{comb} is proportional to $(l_e^2 + r_e^2)(l_\tau^2 - r_\tau^2)$. Thus, while the isolation of events with a final state τ in a definite helicity state would enhance both, the use of polarised beams will only enhance A_{UD} . Hence in this section, we concentrate on the improvement in sensitivity to $\Re(\tilde{b}_Z)$ (which is probed by A_{UD}).

The up-down(UD) asymmetry for τ^- 's in negative helicity state, with negatively polarized e^- and positively polarized e^+ beams (i.e. the polarisation state 'a' as mentioned in Sec. 4.2) is given by

$$A_{UD}^{-,+}(R1; \tau_L) = \frac{-5.66 \Re(\tilde{b}_Z)}{0.836}. \quad (37)$$

Once again, assuming that τ_L 's can be isolated with an efficiency of 40% (20%), the associated 3σ limits on $\Re(\tilde{b}_Z)$ from this single measurement alone for an integrated luminosity $L = 200 \text{ fb}^{-1}$

(i.e. using only part of the data available for option (ii) of the luminosity divide) reads

$$|\Re(\tilde{b}_Z)| \leq \begin{cases} 0.054 & \text{for 40\% efficiency} \\ 0.077 & \text{for 20\% efficiency.} \end{cases} \quad (38)$$

Comparing this to Table 4, the large gain in sensitivity is obvious. And that too with only part of the data. This is significantly better than the maximal sensitivity available for unpolarized beams, namely $|\Re(\tilde{b}_Z)| \leq 0.067$ obtainable for the e^+e^-H final state with $R2$ -cut and isolating τ -helicities with a 40% efficiency. Once the data for the other combinations of beam polarizations and the τ -helicity, viz.

$$\begin{aligned} A_{UD}^{+,-}(R1; \tau_L) &= \frac{4.1 \Re(\tilde{b}_Z)}{0.627}. \\ A_{UD}^{-,+}(R1; \tau_R) &= \frac{4.17 \Re(\tilde{b}_Z)}{0.617}. \\ A_{UD}^{+,-}(R1; \tau_R) &= \frac{-3.02 \Re(\tilde{b}_Z)}{0.462}. \end{aligned} \quad (39)$$

are taken into account (using a χ^2 test), one obtains, for a 40% isolation efficiency,

$$|\Re(\tilde{b}_Z)| \leq \begin{cases} 0.032 & \text{for option (i)} \\ 0.040 & \text{for option (ii) ,} \end{cases} \quad (40)$$

with the numbers for an isolation efficiency of 20% being a little worse. The combined use of beam polarisation and τ -helicity measurement thus plays a very productive role,

To summarize the entire section, we have demonstrated that the CP-odd and \tilde{T} -odd ZZH couplings can be probed far better by the use of polarised beams and/or the information of final state polarisation. The sensitivity to CP-even and \tilde{T} -even anomalous ZZH couplings, (Δa_Z and $\Re(b_Z)$), on the other hand, show only a marginal improvement in their sensitivity limits. However, use of polarised beams helps to constrain these couplings independent of each other.

5 Beam Polarization and the WWH Couplings

A study of the anomalous WWH couplings is possible via the process $e^+e^- \rightarrow \nu\bar{\nu}H$. However, since it receives contributions from both the t -channel WW fusion diagram and the s -channel Bjorken diagram, this determination needs knowledge of the anomalous ZZH couplings, which fortunately, can be measured well from measurements of other final states. It may be argued that, for completely polarized e^\pm beams, the cross section σ_{LR} gets contribution from both the Bjorken and fusion diagrams, whereas only the first contributes to σ_{RL} , and hence it should be possible to use cross sections with different polarisation combinations to reduce the contamination due to the anomalous ZZH couplings. It should be noted however, that in realistic situations one would not have 100% beam polarisation, and thus this effect cannot be entirely neutralized.

Apart from this possible contamination, the determination of WWH anomalous coupling suffers from one more limitation. The presence of a pair of neutrinos deprives us of the full knowledge of the momenta of the final state fermions and, thus, does not allow construction of \tilde{T} -odd observables. Total rates and forward-backward asymmetry with respect to polar angle of

the Higgs boson (each for different combinations of beam polarisations) are the only observables available in the present case. Using the notation of Eq. 14 for the polarisation states, the states ‘*c*’ and ‘*d*’ do not contribute to the process $e^+ e^- \rightarrow \nu \bar{\nu} H$, for the case of 100% polarisation. Even with the assumed values of 80% and 60% polarisation for the e^- and e^+ beams respectively, these two combinations will correspond to rather small cross sections. Therefore, we restrict ourselves to the data accrued from the other two polarisation combinations viz. *a* and *b*. On imposition of the $R1'$ - or the $R2'$ -cut, the cross sections are now given by⁵

$$\begin{aligned}
\sigma^{-,+}(R1'; \nu) &= [9.09 + 17.6 \Delta a_Z + 0.60 \Re(\Delta a_W) + 83.8 \Re(b_Z) - 3.62 \Im(b_Z) \\
&\quad - 0.48 \Im(\Delta a_W) + 0.90 \Re(b_W) + 1.51 \Im(b_W)] \text{ fb} \\
\sigma^{+,-}(R1'; \nu) &= [6.63 + 13.2 \Delta a_Z + 0.02 \Re(\Delta a_W) + 63.4 \Re(b_Z) - 0.10 \Im(b_Z) \\
&\quad - 0.01 \Im(\Delta a_W) + 0.03 \Re(b_W) + 0.04 \Im(b_W)] \text{ fb} \\
\sigma^{-,+}(R2'; \nu) &= [102 - 0.45 \Delta a_Z - 17.6 \Re(b_Z) - 0.31 \Im(b_Z) \\
&\quad + 205 \Re(\Delta a_W) - 38.3 \Re(b_W)] \text{ fb} \\
\sigma^{+,-}(R2'; \nu) &= [3.23 + 0.78 \Delta a_Z + 4.31 \Re(b_Z) + 5.68 \Re(\Delta a_W) - 1.06 \Re(b_W)] \text{ fb}
\end{aligned} \tag{41}$$

That the WWH couplings make a small contribution for the $(+, -)$ case is easy to understand. Furthermore, the contributions from $\Im(b_{W,Z})$ are small as these have to be proportional to the absorptive part of the Z -propagator in Bjorken diagram. As can be expected, the sensitivity to the WWH couplings is enhanced if one can successfully eliminate the contribution of the Z -diagram (this has the further advantage of eliminating the ν_μ and ν_τ events). However, since even the $R2'$ -cut (see Eq. 5) cannot eliminate the Z diagram entirely, as is seen from Eq. 41, we consider a particular linear combination of the cross sections, namely

$$\begin{aligned}
\mathcal{O}_{2\nu_A} &\equiv \sigma^{-,+}(R2'; \nu) + 4 \sigma^{+,-}(R2'; \nu) \\
&= [\eta_1 + 115 + 228 \Re(\Delta a_W) - 42.5 \Re(b_W)] \text{ fb}, \\
\eta_1 &\equiv 2.66 \Delta a_Z - 0.36 \Re(b_Z) - 0.31 \Im(b_Z).
\end{aligned} \tag{42}$$

Thus the contamination from ZZH couplings is contained entirely in η_1 . Using the analysis of the previous section (which did not involve the $\nu \bar{\nu} H$ final state), we have $|\eta_1| \leq 0.13(0.14)$ respectively for options (i) and (ii) of the luminosity division (Eqs. 15). In other words, the uncertainty due to a lack of precise knowledge of the ZZH couplings is reduced to negligible proportions enabling us to constrain a combination of $\Re(\Delta a_W)$ and $\Re(b_W)$ virtually independent of ZZH couplings:

$$|2 \Re(\Delta a_W) - 0.37 \Re(b_W)| \leq 0.040 (0.036) \tag{43}$$

for the two choices of luminosity division among different polarisation modes concerned (see Fig. 4). The relatively small difference between the sensitivities indicates that the luminosity division is not very crucial as long as a sufficiently large fraction is devolved into the canonical choices of $(+, -)$ and $(-, +)$. It may be also noted here that due to large value of SM cross section, the fluctuation in the cross section with $R2'$ -cut given by Eq. 6 is dominated by the systematic error as mentioned in Sec. 3. Thus small changes in luminosity or cross section is

⁵ As stated earlier in Sec. 2, we may choose a_Z to be real, without any loss of generality. But once we make this choice, all the WWH couplings (including Δa_W) may be complex.

not going to make much difference to the sensitivity limits of the couplings that are probed by cross section $\sigma^{-,+}(R2'; \nu)$ or $\mathcal{O}_{2\nu_A}$.

While it is true that we can only probe a combination of these two couplings using $\mathcal{O}_{2\nu_A}$, use of beam polarization clearly helps to reduce contamination from ZZH couplings to this determination. It is to be noted that since only a particular linear combination of $\Re(\Delta a_W)$ and $\Re(b_W)$ can be probed, limits on them are strongly correlated. Of course, it is possible to derive a constraint on the orthogonal combination from the data of Eq. 41, but it is too weak to be of any relevance. If we make a further assumption of only one of these couplings being non-zero, we would obtain

$$\begin{aligned} |\Re(\Delta a_W)| &\leq 0.020 \text{ (0.018)} && \text{for } \Re(b_W) = 0 \\ |\Re(b_W)| &\leq 0.110 \text{ (0.095)} && \text{for } \Re(\Delta a_W) = 0 \end{aligned} \quad (44)$$

with the two limits corresponding to options (i) and (ii) of Eqs. 15. Although a comparison with the results obtained earlier [34] shows only a marginal improvement in the individual limits, the determination is now free of uncertainty coming from contamination from the ZZH couplings.

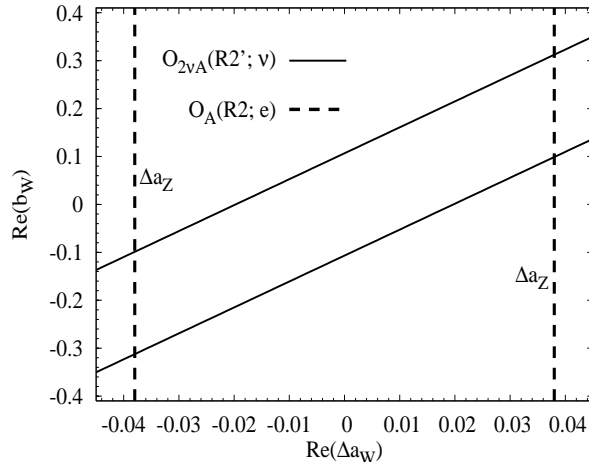


Figure 4: *The region in the $\Re(\Delta a_W) - \Re(b_W)$ plane consistent with 3σ variations in $\mathcal{O}_{2\nu_A}$ for an integrated luminosity of 125 fb^{-1} . The vertical line shows the sensitivity limit on Δa_Z from Fig. 1*

At this stage, it is intriguing to consider the consequences of an additional assumption (made in Ref. [34]) of $\Delta a_W = \Delta a_Z$, which is found to be true in some cases [71] and would be motivated by $SU(2) \times U(1)$ invariance of the effective theory. By itself, this would impose a bound on Δa_W , courtesy Eq. 17 and hence that would lead to a closed area as shown in Fig. 4. However, one should also note that $SU(2) \times U(1)$ invariance would further equate b_W and b_Z , and that the correlation between constraints in the $\Re(b_W) - \Re(\Delta a_W)$ plane (Fig. 4) is in the opposite sense to that in the $\Re(b_Z) - \Delta a_Z$ plane (Fig. 1). Thus, an assumption of such an invariance would lead to far stronger constraints. In particular, the improvement is dramatic for $\Re(b_W)$.

As for the other CP-even WWH couplings, namely $\Im(\Delta a_W)$ and $\Im(b_W)$, note that their contributions arise from the interference of the WW -fusion diagram with the absorptive part

of the Z -propagator in the Bjorken diagram. Hence the corresponding terms appear only in total rate with $R1'$ -cut and being proportional to the width of Z -boson, are very small. Since the presence of two neutrinos in the final state does not allow us to construct any \tilde{T} -odd observables, this study is virtually insensitive to these two couplings. Of course, an assumption of $SU(2) \times U(1)$ invariance would change matters drastically.

What remains is to investigate \tilde{b}_W , and this being a CP-odd coupling, can be probed through the forward-backward (FB) asymmetry with respect to the polar angle of Higgs boson. These asymmetries, $R1'$ - or and $R2'$ -cuts can be expressed as

$$\begin{aligned}
A_{FB}^{-,+}(R1'; \nu) &= \frac{1}{9.09} \left[-2.29 \Re(\tilde{b}_Z) - 36.9 \Im(\tilde{b}_Z) + 0.57 \Re(\tilde{b}_W) - 0.47 \Im(\tilde{b}_W) \right], \\
A_{FB}^{+,-}(R1'; \nu) &= \frac{1}{6.63} \left[-0.064 \Re(\tilde{b}_Z) + 27.1 \Im(\tilde{b}_Z) + 0.02 \Re(\tilde{b}_W) - 0.01 \Im(\tilde{b}_W) \right], \\
A_{FB}^{-,+}(R2'; \nu) &= \frac{1}{102} \left[5.17 \Im(\tilde{b}_Z) + 7.83 \Im(\tilde{b}_W) \right], \\
A_{FB}^{+,-}(R2'; \nu) &= \frac{1}{3.23} \left[2.1 \Im(\tilde{b}_Z) + 0.22 \Im(\tilde{b}_W) \right].
\end{aligned} \tag{45}$$

where the numbers once again represent the corresponding cross sections in femtobarns. With the last two of Eqs. 45 involving just a single WWH coupling, these can be combined to eliminate the remaining dependence on the ZZH anomalous couplings to leave us

$$\begin{aligned}
A_{2_{\text{mix}}} &\equiv 13 A_{FB}^{-,+}(R2'; \nu) - A_{FB}^{+,-}(R2'; \nu) \\
&= 0.009 \Im(\tilde{b}_Z) + 0.93 \Im(\tilde{b}_W).
\end{aligned} \tag{46}$$

The contribution to $A_{2_{\text{mix}}}$ from $\Im(\tilde{b}_Z)$ (which, incidentally, can be probed very accurately, see Table 4) may be neglected, leading to

$$|\Im(\tilde{b}_W)| \leq 0.50 \quad (0.44) \tag{47}$$

for $\mathcal{L} = 125 \text{ (200) fb}^{-1}$ for each of the $(+, -)$ and $(-, +)$ polarization combinations. While it may seem that the improvement is marginal when compared to the sensitivity achievable with unpolarised beams— $|\Im(\tilde{b}_W)| \leq 0.46$ for a total luminosity of 500 fb^{-1} [34]—note that, unlike the older analysis, the current sensitivity is independent of any other coupling. In other words, the use of beam polarisation has allowed construction of an observable that can isolate the contribution of $\Im(\tilde{b}_W)$.

The anomalous coupling $\Re(\tilde{b}_W)$ being a \tilde{T} -odd coupling has no contribution to FB asymmetries with $R2'$ -cut and only a small contribution to FB asymmetries with $R1'$ -cut through the interference of the WW -fusion diagram with the absorptive part of Bjorken diagram. Hence these asymmetries are not a good probe of $\Re(\tilde{b}_W)$. Thus the process under consideration can not be used to probe any of the \tilde{T} -odd couplings in the WWH vertex.

To summarize the results of this section: use of beam polarisation allows us to obtain limits on \tilde{T} -even couplings $\Re(\Delta a_W)$, $\Re(b_W)$ and $\Im(\tilde{b}_W)$ *independent* of the ZZH couplings, these being listed in Table 6. Using linear combinations of our observables corresponding to different polarisation combinations for initial states, the contamination from ZZH coupling can be reduced to negligible amount, something that was not possible with the unpolarised beams. Further, even though this measurement uses only two of the combinations, an equal division of

Using Polarized Beams			Unpolarized States		
Coupling	Limits (for given \mathcal{L})		Observables used	Limits	Observables used
	200 fb ⁻¹	125 fb ⁻¹			
$ \Re(\Delta a_W) \leq$	0.018	0.020	$\mathcal{O}_{2\nu_A}$	0.019	$\sigma^{unpol}(R2'; \nu)$
$ \Re(b_W) \leq$	0.095	0.11	$\mathcal{O}_{2\nu_A}$	0.10	$\sigma^{unpol}(R2'; \nu)$
$ \Im(\tilde{b}_W) \leq$	0.44	0.50	$A_{2\text{mix}}$	0.40	$A_{FB}^{unpol}(R2'; \nu)$

Table 6: 3σ limits on anomalous WWH couplings from various observables with polarized and unpolarized beams.

the total luminosity among all four already gives optimal results. The limits on $\Re(\Delta a_W)$ and $\Re(b_W)$ are highly correlated whereas $\Im(\tilde{b}_W)$ is constrained independent of any other coupling. There is no observable to constrain the \tilde{T} -odd couplings and thus we conclude that this process is not a good probe for these couplings. Hence one has to look to other processes to probe these couplings. For example, this problem may be overcome in the $e\gamma$ collider as shown in Ref. [72]. The WWH couplings are not contaminated by the ZZH couplings in the process studied there viz. ($e^-\gamma \rightarrow \nu W^- H$). Using this process in conjunction with the $P\tilde{T}$ conjugate process, the authors were able to construct observables that depend only on one of the anomalous WWH couplings and hence the limits obtained on each of the WWH couplings were independent of the others. The anomalous VVH couplings at $e\gamma$ collider have been also studied in Ref. [73]. Finally, an assumption of $SU(2) \times U(1)$ invariance would drastically improve the constraints for virtually all the couplings, whether they be WWH or ZZH .

6 Dependence on \sqrt{s} and inclusion of ISR/Beamstrahlung Effects

All our analysis so far has been performed for a fixed centre of mass energy, namely $\sqrt{s} = 500$ GeV. Clearly, the total cross section is a function of energy, and the functional form may depend on the presence of (and the identity of) any anomalous coupling, owing to their higher-dimensional nature. Thus, the sensitivities could, in principle, depend on the choice of \sqrt{s} . Furthermore, for the processes involving both s - and t -channel diagrams, the relative importance of these two parts of the amplitude is, in fact, energy dependent, and the generic enhancement of the t -channel cross section with increasing beam energies may, in principle, lead to an improvement in the sensitivity to those couplings primarily constrained using observables with $R2$ -($R2'$)-cut.

Even for a nominally fixed beam energy, the \sqrt{s} available to an individual hard scatter-

ing event is generically less than this value owing to the ubiquitous initial state radiation (ISR)—which is nothing but the bremsstrahlung radiation by the incoming particles—or beamstrahlung, which is a name for the radiation from the beam particles due to its interaction with the (strong) electromagnetic fields caused by the dense bunches of the opposite charge in a collider environment. Consequently, it is important to investigate the possibly detrimental effects of such eventualities.

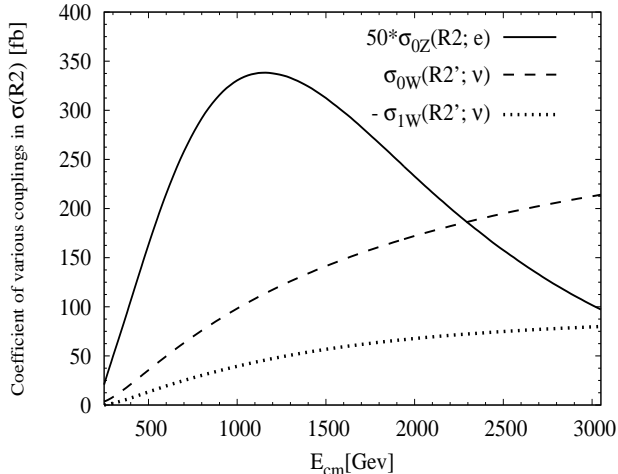


Figure 5: \sqrt{s} -variation of $(\sigma_{0Z}(R2; e)$ (the SM part in the cross section $\sigma(R2; e) = \sigma(e^+e^- \rightarrow e^+e^-H)$ with $R2$ -cut), $\sigma_{0W}(R2'; \nu)$ and $\sigma_{1W}(R2'; \nu)$ (the coefficients of $\Re(\Delta a_W)$ and $\Re(b_W)$ respectively in the cross section for $e^+e^- \rightarrow \nu\bar{\nu}H$ with $R2'$ -cut).

To this end, we begin by studying the \sqrt{s} -dependence of the observables used in this paper. For simplicity, we shall restrict ourselves, in this section, to unpolarised scattering, with the results for polarised beams expected to be similar. Moreover, we shall concentrate on observables defined with the $R2$ -($R2'$)-cut. For example, the ZZH coupling Δa_Z is best probed by the total cross section with $R2$ -cut for electron final state i.e. $\sigma(R2; e) = \sigma(e^+e^- \rightarrow e^+e^-H)$ with $R2$ -cut. Fig. 5 shows the variation of the SM part of this cross section (σ_{0Z} of Eq. 7) with \sqrt{s} .⁶ Recall that Δa_Z simply rescales the SM part of the cross section (Eq. 7) and hence the sensitivity is determined simply by the corresponding number of events, namely it scales as $N_{0Z}^{-1/2}$. With $\sigma_{0Z}(R2; e)$ having a maximum at $\sqrt{s} \approx 1.1$ TeV, this would be the optimal beam energy to probe Δa_Z , with the maximal improvement (compared to the results quoted above) being by about 40%.

Fig. 5 also shows the \sqrt{s} -variation of the SM and $\Re(b_W)$ contributions (i.e. σ_{0W} and σ_{1W} respectively) to the cross section $\sigma(R2'; \nu) = \sigma(e^+e^- \rightarrow \nu\bar{\nu}H)$ with $R2'$ -cut which is the best probe for the WWH couplings $\Re(\Delta a_W)$ and $\Re(b_W)$. While the monotonic increase in σ_{1W} would seem to suggest that increasing \sqrt{s} would readily lead to an improvement in the sensitivity to $\Re(b_W)$, note that this increase saturates and, furthermore, that σ_{0W} increases at least as fast. Consequently, for moderate changes in \sqrt{s} , any improvement or otherwise is expected to be marginal at best.

⁶Note that σ_{0Z} has been scaled by a factor of 50 to fit in the same figure.

Moving to asymmetries, the up-down asymmetry $A_{UD}(R2; e)$ of the final state fermion with respect to the H -production plane, and the forward-backward asymmetry with respect to polar angle of the Higgs boson, $A_{FB}(R2'; \nu)$ have been used to constrain $\Re(\tilde{b}_Z)$ and $\Im(\tilde{b}_W)$ respectively [34]. Expressing these as

$$\begin{aligned} A_{UD}(R2; e) &= A_{UD}^a \Re(\tilde{b}_Z) \\ A_{FB}(R2'; \nu) &= A_{FB}^b \Im(\tilde{b}_Z) + A_{FB}^c \Im(\tilde{b}_W) \end{aligned} \quad (48)$$

the coefficients A_{UD}^a and A_{FB}^c are plotted in Fig. 6 as a function of \sqrt{s} . The figure clearly shows

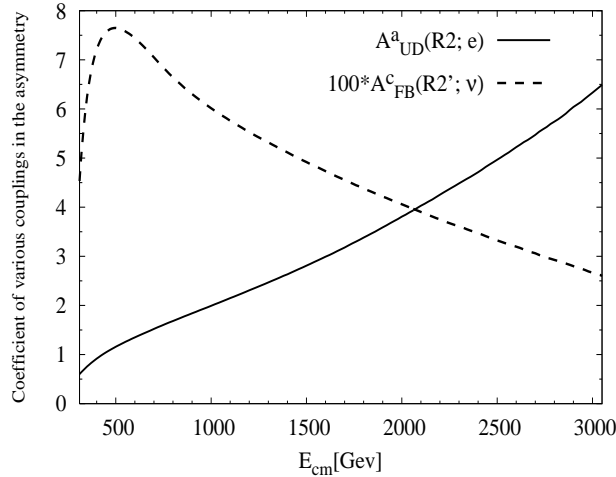


Figure 6: \sqrt{s} -variation of the coefficients A_{UD}^a in up-down asymmetry and the A_{FB}^c in forward-backward asymmetry as defined in Eq. 48 of the text. Both plots are with R2-(R2')-cut (de-selecting Z pole) imposed.

that the sensitivity to $\Re(\tilde{b}_Z)$ is expected to improve at higher \sqrt{s} , while, $\sqrt{s} = 500$ GeV is an optimal choice for $\Im(\tilde{b}_W)$ and higher energies would only tend to deteriorate the sensitivity. The arguments above are reflected by Table 7 which summarizes the sensitivity limits at the 3σ level, with an integrated luminosity of 500 fb^{-1} , for different center of mass energies.

The above analysis did not take into account either of ISR and beamstrahlung. We now proceed to do so, using the structure function formalism [48] to incorporate these effects. The differential scattering cross section for a given process $e^-(p_1) + e^+(p_2) \rightarrow X(\gamma)$ can be expressed as:

$$d\sigma[e^+e^- \rightarrow X(\gamma)] = f_{e/e}(x_1) f_{e/e}(x_2) d\hat{\sigma}[e^+e^- \rightarrow X](\hat{s}) ,$$

where the electron luminosity function $f_{e/e}(x)$ describes the probability of finding an electron with a momentum fraction x of the nominal beam energy, or, in other words, the probability with which an electron energy $E = \sqrt{s}/2$ emits one or more photons with total energy $(1-x)E$ resulting in the reduction of its energy to $E_e = xE$. Hence the square of the effective c.m. energy \hat{s} can be expressed as: $\hat{s} \simeq x_1 x_2 s$.

Using the Weiszäcker-Williams approximation, one can write down the luminosity function for ISR as [47]

$$f_{e/e}^{\text{ISR}}(x) = \frac{\beta}{16} \left[(8 + 3\beta)(1-x)^{\beta/2-1} - 4(1+x) \right] , \quad (49)$$

Coupling		3 σ limit at $\sqrt{s} = 0.5$ TeV	3 σ limit at $\sqrt{s} = 1$ TeV	3 σ limit at $\sqrt{s} = 3$ TeV	Observable used
$ \Delta a_Z \leq$		0.040	0.030	0.049	$\sigma(R2; e)$
		0.043	0.031	0.039	$\sigma^{\text{ISR+Beam.}}(R2; e)$
$ \Re(\tilde{b}_Z) \leq$		0.067	0.028	0.015	$A_{UD}(R2; e)$
		0.075	0.032	0.018	$A_{UD}^{\text{ISR+Beam.}}(R2; e)$
$ \Re(\Delta a_W) \leq$		0.019	0.016	0.016	$\sigma(R2'; \nu)$
		0.019	0.017	0.016	$\sigma^{\text{ISR+Beam.}}(R2'; \nu)$
$ \Re(b_W) \leq$		0.10	0.082	0.084	$\sigma(R2'; \nu)$
		0.11	0.084	0.083	$\sigma^{\text{ISR+Beam.}}(R2'; \nu)$
$ \Im(\tilde{b}_W) \leq$		0.40	0.42	0.89	$A_{FB}(R2'; \nu)$
		0.43	0.41	0.71	$A_{FB}^{\text{ISR+Beam.}}(R2'; \nu)$

Table 7: *Individual sensitivity limits (assuming only the relevant coupling to be non-zero) at the 3σ level for an integrated luminosity of 500 fb^{-1} on various anomalous couplings at different c.m. energies without and with the inclusion of ISR and beamstrahlung effects. The results correspond to unpolarised beams.*

where

$$\beta = \frac{2\alpha_{em}}{\pi} \left(\log \frac{s}{m_e^2} - 1 \right), \quad (50)$$

and α_{em} is the fine-structure constant.

The beamstrahlung spectrum depends on electron beam energy E , and the parameters such as the number of electrons per bunch N_e , the bunch dimensions (for a Gaussian bunch profile) in both the longitudinal direction (σ_z) as well as in the transverse directions ($\sigma_{y,x}$). It is convenient to introduce a ‘‘beamstrahlung parameter’’ Υ [49] given by:

$$\Upsilon = \frac{5 r_e^2 E N_e}{6 \alpha_{em} \sigma_z (\sigma_x + \sigma_y) m_e},$$

where r_e is the classical electron radius, and m_e its mass. The electron spectrum $f_{e/e}^{\text{beam}}(x)$ describing the effects of beamstrahlung, can be written in a closed analytical form for $\Upsilon \lesssim 10$ [49]. Armed with all these, the expression for the electron spectrum function, including both ISR and beamstrahlung effects, may be written as [48]:

$$f_{e|e}(x) = \int_x^1 \frac{d\xi}{\xi} f_{e|e}^{\text{ISR}}(\xi) f_{e|e}^{\text{beam}}(\xi^{-1} x), \quad (51)$$

where $f_{e|e}^{\text{ISR}}(\xi)$ is as given in Eq. 49 above, whereas $f_{e|e}^{\text{beam}}(\xi^{-1}x)$ is that given by Eq. 22 of Ref. [49].

We now analyse how the ISR and beamstrahlung effects modify the sensitivity limits of $\Re(\tilde{b}_Z)$, for which we had observed an improvement in sensitivity at higher \sqrt{s} as listed in Table 7. In our analysis we use the beamstrahlung parameters to be [74]

$$\begin{aligned} \sigma_z &= 30 \mu\text{m} \text{ for all energies,} \\ \Upsilon &= 0.3, 1.0 \text{ and } 8.1 \text{ for } E_{\text{cm}} = 0.5, 1.0, \text{ and } 3.0 \text{ TeV respectively.} \end{aligned} \quad (52)$$

Fig. 7 compares the total rates with and without ISR effect for different final states. The

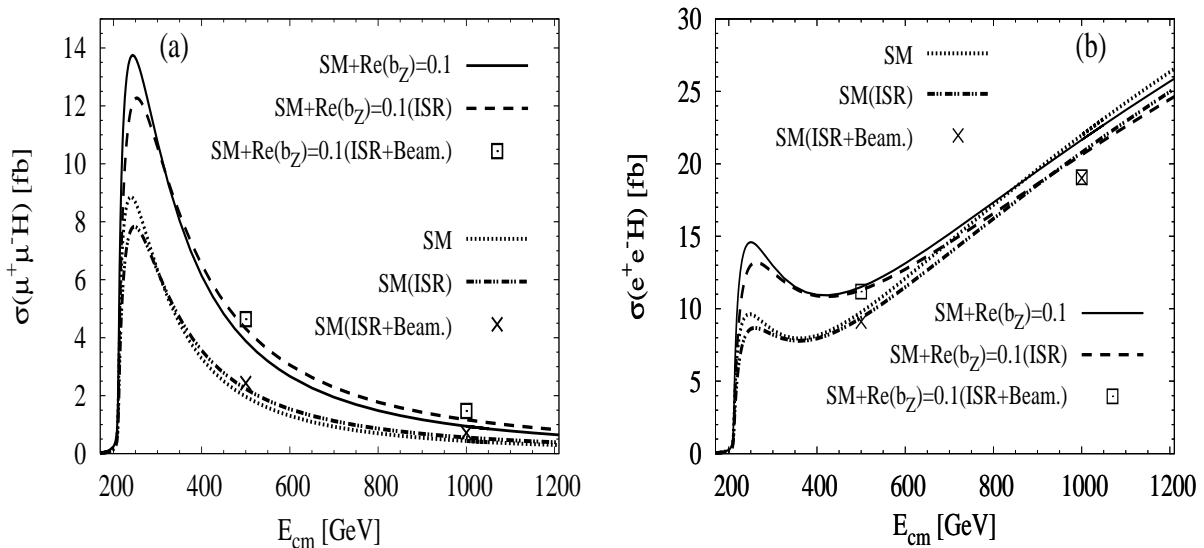


Figure 7: \sqrt{s} -variation of cross sections with and without the ISR effects for final states with muons or electrons. The figure also shows the points at $\sqrt{s} = 0.5$ TeV and 1.0 TeV when beamstrahlung effects are also included. Beamstrahlung effects are negligible at $\sqrt{s} = 0.5$ TeV.

effective c.m. energy \hat{s} of the electron beam decreases due to ISR. As a result, away from the threshold, the ISR effects increase the rates of pure s -channel processes, such as $e^+ e^- \rightarrow \mu^+ \mu^- H$. Near the threshold, however, the cross section rises with the effective \sqrt{s} and hence the ISR effects cause a decrease in the rate. For the process under discussion, the cross-over from one behaviour to the other takes place at about 300 GeV. On the other hand, $(e^+ e^- H)$ -production receives both s - and t -channel contributions, and hence there is no such cross-over with ISR effects always decreasing the rates. We thus expect these effects to reduce somewhat the improvement observed above in probing $\Re(\tilde{b}_Z)$ at higher energies.

At $\sqrt{s} = 500$ GeV, beamstrahlung effects are negligible whereas ISR effects cause 10% to 15% change in cross section (see Fig. 7). However, this does not cause significant changes in sensitivities as both the SM and anomalous parts are affected in much the same way. At higher c.m. energies both ISR and beamstrahlung effects are nontrivial and significant. However, once again, the effect is in the same direction, and roughly of the same magnitude, for the SM and in the presence of anomalous couplings (Fig. 7). Although the figure demonstrates this for total cross sections, the story is similar even for partial cross sections and for the other couplings as well.

Since the constraints on $\Re(\tilde{b}_Z)$ are the only ones to improve significantly with increasing \sqrt{s} (see Table 7), we concentrate on the effects of ISR and beamstrahlung on this coupling. With $\Re(\tilde{b}_Z)$ being best probed by the up-down asymmetry (with $R2$ -cut) for electrons in (e^+e^-H) production, the ISR and beamstrahlung effects can be summarised as listed in Table 8.

\sqrt{s}	UD-asymmetry($A_{UD}(R2; e)$)		
	No ISR & Beam.	With ISR	With ISR & Beam.
0.5 TeV	1.16 $\Re(\tilde{b}_Z)$	1.13 $\Re(\tilde{b}_Z)$	1.1 $\Re(\tilde{b}_Z)$
1 TeV	2.00 $\Re(\tilde{b}_Z)$	1.94 $\Re(\tilde{b}_Z)$	1.85 $\Re(\tilde{b}_Z)$
3 TeV	6.29 $\Re(\tilde{b}_Z)$	5.60 $\Re(\tilde{b}_Z)$	4.23 $\Re(\tilde{b}_Z)$

Table 8: *Up-down asymmetry for final state electron for $R2$ -cut($A_{UD}(R2; e)$) with and without ISR and beamstrahlung effects at different \sqrt{s} 's.*

As is readily seen, the effects are almost negligible even for $\sqrt{s} = 1$ TeV, and only marginally important for $\sqrt{s} = 3$ TeV. The consequent shift in the sensitivities are summarised in Table 7. The smallness of the effects can be understood by realizing that, on the imposition of the $R2$ -cut (de-selecting the Z -pole), the energy dependence of the cross sections (total or partial) is only logarithmic. Further, both SM and anomalous parts have a similar dependence. Hence although the cross sections are affected significantly there is little effect on the sensitivity limits of the anomalous parts after inclusion of ISR and beamstrahlung effects.

We conclude this section by making a few general observations :

- With increasing energy, the observables with the $R2$ -cut imposed gain more in sensitivity as compared to those defined with the $R1$ -cut.
- Observables with $R1$ -cut (selecting Z -pole) are affected more by ISR and beamstrahlung corrections because of the usual s -channel suppression, whereas the observables with $R2$ -cut (de-selecting Z -pole) have only logarithmic \sqrt{s} -dependence and hence do not suffer as significant corrections.
- By using higher c.m. energies, we gain significantly in the sensitivity to $\Re(\tilde{b}_Z)$ (upto a factor of 2 at $\sqrt{s} = 1$ TeV as compared to the case of 500 GeV). Neither the ISR nor the beamstrahlung effects change the sensitivity significantly.
- There is no significant gain in the sensitivity to anomalous WWH couplings even at very high energies.
- In totality, we do not gain much in the sensitivity by going to higher c.m. energies. Thus, running the collider at lower energies (say $\sqrt{s} = 500$ GeV), but with polarised beams is more beneficial for the study of anomalous VVH couplings.

7 Summary

With the plethora of the gauge boson couplings with a Higgs that an effective theory allows, it is always going to be a complicated task to unravel these. It was shown in Ref. [34] that it is possible to construct observables with definite CP and \tilde{T} transformation properties that are sensitive to a single anomalous coupling (the one with matching CP and \tilde{T} properties) and hence these observables may be used to obtain robust constraints on the couplings in a model independent way. With polarised beams, we have the possibility of constructing even more such observables.

We have performed our analysis by imposing kinematical cuts on different final state particles to reduce backgrounds. In addition, we also include the reduction (in the event rates) caused by considering only the events wherein the H decays into a $b\bar{b}$ pair (with branching fraction ~ 0.68), with a realistic b -tagging efficiency of 70%. This renders, to a great extent, our estimates of sensitivity quite realistic.

Almost all of the asymmetries pertaining to the probe of the ZZH vertex, that were constructed in Ref. [34] for unpolarised beams and neglecting the polarisation of the final state particles, are proportional to the difference between the squared right and left handed coupling of the Z to charged leptons. Consequently, one expects the sensitivity to the corresponding anomalous couplings to be enhanced once one uses a specific polarisation, thereby overcoming this cancellation between the (almost) equal left and right handed couplings of the Z boson to leptons. Indeed, we observe this. For example, the use of beam polarization alone leads on the one hand, to the disentangling of the couplings Δa_Z and $\Re(b_Z)$ (not possible for unpolarised beams), and on the other, to an improvement in the sensitivities to CP -odd ZZH couplings by a factor of upto 5-7.

With the helicity of a τ in the final state decipherable from the momentum distribution of the charged prongs in its decay, one can construct asymmetries pertaining to τ 's with a specific helicity. Assuming that it would be possible to isolate events with τ 's in a definite helicity state with an efficiency of (say) 40%, we use such asymmetries to demonstrate that sensitivity to $\Im(b_Z)$ and $\Re(\tilde{b}_Z)$ could be improved by a factor of about 3. While an earlier optimal observable analysis [31] had indeed investigated the use of τ helicity, our analysis differs in that we have constructed an observable that can be measured in a simple counting experiment and catches the essence of the optimal observable. Also worth noting is that the use of final state τ measurement along with polarised beams, allows us to improve on the sensitivity for $\Re(\tilde{b}_Z)$ by a factor of about 2.

As far as the constraints on the anomalous WWH couplings are concerned, the problem of a smaller number of observables due to the presence of missing neutrinos in the the $\nu\bar{\nu}H(b\bar{b})$ still exists. However, by constructing new observables that are combinations of the observables corresponding to different polarisation states, the contamination from the anomalous ZZH couplings is highly reduced in case of \tilde{T} -even WWH couplings which is a great advantage over the use of unpolarised beams. For \tilde{T} -odd WWH couplings though, we conclude that this process is not a good probe for them because of non-availability of any \tilde{T} -odd observable. Hence one has to look to other processes to probe these couplings.

We have also investigated possible gains in sensitivity by going to higher centre of mass energies. This though renders ISR and the beamstrahlung effects progressively more important. As a matter of fact, even for $\sqrt{s} = 500$ GeV, the ISR effects can affect cross sections with the $R1$ -cut by 10–15%. Fortunately, the ISR and beamstrahlung effects on sensitivity limits is very

modest, as both the standard model and the anomalous contributions change by similar amounts causing only small numerical effects, especially on the asymmetries. As for the variation in sensitivity with \sqrt{s} ranging from 300 GeV to 3 TeV, the observables with the $R1$ -cut (selecting the Z -pole) are naturally associated with a larger cross section (and, hence, better limits) for lower energies. Thus, a machine operating at $\sqrt{s} = 350$ GeV would do even better for certain couplings than the present case. This is in agreement with the findings of Ref. [34]. For observables constructed with the $R2$ -cut, however, one can obtain an improvement in the sensitivity limit (say) for $\Re(\tilde{b}_Z)$ by upto a factor of 2 at c.m. energy 1 TeV compared to the ones possible at 500 GeV [34].

In conclusion, we find that use of beam polarisation and final state τ polarisation can result in significant advances in the search for anomalous ZZH couplings at the ILC. For WWH couplings, though there is no significant change in the sensitivity limits, the \tilde{T} -even ones can be now probed virtually independent of the anomalous ZZH couplings. The inclusion of ISR and beamstrahlung effects, changes the individual cross sections but has very little effect on the sensitivities. Further, going to higher beam energies, leads to only modest improvements. Thus, as far as this sector of the theory is concerned, there is a strong case for use of beam polarisation and measurement of final state fermion polarisations wherever possible, but there is no real gain in going to higher energies.

Acknowledgments

We thank R. K. Singh for collaboration in the initial phase of this project. DC & M acknowledge partial support from the Department of Science and Technology(DST), India under grants SR/S2/RFHEP-05/2006 and SR/S2/HEP-12/2006 respectively and infrastructural support from the IUCAA Reference Centre, Delhi. R.M.G. wishes to acknowledge the DST under Grant No. SR/S2/JCB-64/2007. RMG also wishes to acknowledge support from the Indo French Centre for Promotion of Advanced Scientific Research under project number 3004-2.

Note: During the last stages of finalising our manuscript, a paper dealing with related issues containing a very detailed analysis [75] on probing the coefficients of the CP-even, dimension 6 operators in the anomalous VVH vertices has appeared.

References

- [1] P.W. Higgs, Phys. Rev. Lett. 13 (1964) 508; Phys. Rev. 145 (1966) 1156; F. Englert and R. Brout, Phys. Rev. Lett. 13 (1964) 321; G.S. Guralnik, C.R. Hagen and T. Kibble, Phys. Rev. Lett. 13 (1964) 585.
- [2] J. Gunion, H. Haber, G. Kane, and S. Dawson, *The Higgs Hunter's Guide*, Addison–Wesley, Reading (USA), 1990.
- [3] M. Gomez-Bock *et al.*, J. Phys. Conf. Ser. **18**, 74 (2005) [arXiv:hep-ph/0509077].

- [4] A. Djouadi, Phys. Rept. **457**, 1 (2008) [arXiv:hep-ph/0503172]; Phys. Rept. **459**, 1 (2008) [arXiv:hep-ph/0503173].
- [5] For a review, see for example, R. M. Godbole, [arXiv:hep-ph/0205114], Volume 4, Jubilee Issue of the Indian Journal of Physics, pp. 44-83, 2004, Guest Editors: A. Raychaudhuri and P. Mitra.
- [6] ATLAS Collaboration, Technical Design Report, CERN-LHCC-99-14 and CERN-LHCC-99-15; CMS Collaboration, Technical Design Report, CMS-LHCC-2006-21.
- [7] ALEPH, DELPHI, L3 and OPAL Collaborations, The LEP Working Group for Higgs Boson Searches, Phys. Lett. **B565**, 61 (2003); see also <http://lep-higgs.web.cern.ch/LEPHIGGS/>
- [8] LEP Electroweak Working Group, <http://lepewwg.web.cern.ch/LEPEWWG/> J. Alcaraz *et al.* [LEP Collaborations], CERN-PH-EP/2007-039, arXiv:0712.0929 [hep-ex].
- [9] R. Akers *et al.* [OPAL Collaboration], Z. Phys. **C61**, 19 (1994); D. Buskulic *et al.* [ALEPH Collaboration], Z. Phys. **C62**, 539 (1994); M. Acciarri *et al.* [L3 Collaboration], Z. Phys. **C62**, 551 (1994); P. Abreu *et al.* [DELPHI Collaboration], Z. Phys. **C67**, 69 (1995); D. Antreasyan *et al.* [Crystal Ball Collaboration], Phys. Lett. **B251**, 204 (1990); P. Franzini *et al.*, Phys. Rev. **D35**, 2883 (1987); J. Kalinowski and M. Krawczyk, Phys. Lett. **B361**, 66 (1995) [arXiv:hep-ph/9506291]; D. Choudhury and M. Krawczyk, Phys. Rev. **D55**, 2774 (1997) [arXiv:hep-ph/9607271].
- [10] M. Carena, J. R. Ellis, A. Pilaftsis and C. E. M. Wagner, Nucl. Phys. **B586**, 92 (2000).
- [11] A. Mendez and A. Pomarol, Phys. Lett. **B279**, 98 (1992); J. F. Gunion, H. E. Haber and J. Wudka, Phys. Rev. **D43**, 904 (1991); J. F. Gunion, B. Grzadkowski, H. E. Haber and J. Kalinowski, Phys. Rev. Lett. **79**, 982 (1997) [hep-ph/9704410]; I. F. Ginzburg, M. Krawczyk and P. Osland, hep-ph/0211371; I. F. Ginzburg and M. Krawczyk, Phys. Rev. D **72**, 115013 (2005).
- [12] See e.g. M. Drees, R.M. Godbole and P. Roy, *Theory and phenomenology of sparticles*, World Scientific, 2005; H. Baer and X. Tata, “*Weak scale Supersymmetry: From superfields to scattering events*,” Cambridge, UK: Univ. Pr. (2006) .
- [13] G. Abbiendi *et al.* [OPAL Collaboration], Eur. Phys. J. C **37**, 49 (2004) [arXiv:hep-ex/0406057]; ALEPH, DELPHI, L3 and OPAL Collaborations, The LEP Working Group for Higgs Boson Searches, LHWG-Note 2004-01, CERN-PH-EP-2006-001; S. Schael *et al.* [ALEPH Collaboration], Eur. Phys. J. C **47** (2006) 547 [arXiv:hep-ex/0602042].
- [14] E. Accomando *et al.*, Report of “Workshop on CP studies and non-standard Higgs physics,” CERN-2006-009, arXiv:hep-ph/0608079.
- [15] See for example, J. R. Forshaw, Pramana **63**, 1119 (2004) and discussion therein; see also D. Choudhury, T. M. P. Tait and C. E. M. Wagner, Phys. Rev. **D65**, 053002 (2002) [arXiv:hep-ph/0109097].

- [16] E. Accomando *et al.*, Phys. Rept. 299 (1998) 1 [arXiv:hep-ph/9705442]; J. Aguilar-Saavedra *et al.*, hep-ph/0106315; T. Abe *et al.*, hep-ex/0106055-58; K. Abe *et al.*, hep-ph/0109166.
- [17] J. Brau *et al.*, SLAC-R-857; A. Djouadi *et al.*, arXiv:0709.1893 [hep-ph].
- [18] G. Weiglein *et al.* [LHC/LC Study Group], Phys. Rept. **426**, 47 (2006) [arXiv:hep-ph/0410364].
- [19] For a review, see, e.g., R. M. Godbole *et al.*, arXiv:hep-ph/0404024 and references therein.
- [20] V. D. Barger *et al.*, Phys. Rev. D **49** (1994) 79 [arXiv:hep-ph/9306270], A. Skjold and P. Osland, Phys. Lett. B **311** (1993) 261 [arXiv:hep-ph/9303294]; Nucl. Phys. B **453** (1995) 3 [arXiv:hep-ph/9502283].
- [21] A. Djouadi and B. Kniehl, *Correlations in Higgs production and decay as a probe of CP-violation in the scalar sector*, published in the Proceedings of the Workshop on “ e^+e^- Collisions”, Report DESY-93-123C.
- [22] D. J. Miller *et al.*, Phys. Lett. B **505** (2001) 149 [arXiv:hep-ph/0102023].
- [23] M. T. Dova, P. Garcia-Abia and W. Lohmann, arXiv:hep-ph/0302113.
- [24] P. S. Bhupal Dev *et al.*, Phys. Rev. Lett. **100**, 051801 (2008) [arXiv:0707.2878 [hep-ph]]; arXiv:0710.2669 [hep-ph].
- [25] R. M. Godbole and P. Roy, Phys. Rev. Lett. **50** (1983) 717; P. Kalyniak, J. N. Ng, P. Zakarauskas, Phys. Rev. D **29**, 502 (1984), J. C. Romao and A. Barroso, Phys. Lett. B **185**, 195 (1987). W. Kilian, M. Kramer and P. M. Zerwas, Phys. Lett. B **373**, 135 (1996) [arXiv:hep-ph/9512355] and referneces therein.
- [26] K. Hagiwara and M. L. Stong, Z. Phys. C **62** (1994) 99 [arXiv:hep-ph/9309248].
- [27] R. Rattazzi, Z. Phys. C **40** (1988) 605.
- [28] H. J. He, Y. P. Kuang, C. P. Yuan and B. Zhang, Phys. Lett. B **554**, 64 (2003) [arXiv:hep-ph/0211229].
- [29] K. Hagiwara, S. Ishihara, R. Szalapski and D. Zeppenfeld, Phys. Rev. D **48**, 2182 (1993); K. Hagiwara, R. Szalapski and D. Zeppenfeld, Phys. Lett. B **318**, 155 (1993) [arXiv:hep-ph/9308347].
- [30] G. J. Gounaris, F. M. Renard and N. D. Vlachos, Nucl. Phys. B **459**, 51 (1996) [arXiv:hep-ph/9509316].
- [31] K. Hagiwara, S. Ishihara, J. Kamoshita and B. A. Kniehl, Eur. Phys. J. C **14**, 457 (2000) [arXiv:hep-ph/0002043].
- [32] D. Chang, W. Y. Keung and I. Phillips, Phys. Rev. D **48** (1993) 3225 [arXiv:hep-ph/9303226].

- [33] T. Han and J. Jiang, Phys. Rev. D **63**, 096007 (2001) [arXiv:hep-ph/0011271].
- [34] S. S. Biswal, R. M. Godbole, R. K. Singh and D. Choudhury, Phys. Rev. D **73**, 035001 (2006) [Erratum-ibid. D **74**, 039904 (2006)] [arXiv:hep-ph/0509070].
- [35] S. S. Biswal, D. Choudhury, R. M. Godbole and R. K. Singh, Pramana **69**, 777 (2007).
- [36] D. Atwood and A. Soni, Phys. Rev. D **45**, 2405 (1992).
- [37] S. Y. Choi, D. J. Miller, M. M. Muhlleitner and P. M. Zerwas, Phys. Lett. B **553** (2003) 61 [arXiv:hep-ph/0210077].
- [38] C. P. Buszello, I. Fleck, P. Marquard and J. J. van der Bij, Eur. Phys. J. C **32** (2004) 209 [arXiv:hep-ph/0212396]; C. P. Buszello and P. Marquard, in Ref. [14]; C. P. Buszello, P. Marquard and J. J. van der Bij, arXiv:hep-ph/0406181.
- [39] M. Bluj, Acta Phys. Polon. B **38**, 739 (2007).
- [40] R. M. Godbole, D. J. Miller, S. Moretti and M. M. Mühlleitner, Pramana **67** (2006) 617; *ibid.* in Ref. [14].
- [41] B. Zhang, Y. P. Kuang, H. J. He and C. P. Yuan, Phys. Rev. D **67**, 114024 (2003) [arXiv:hep-ph/0303048].
- [42] S. M. Lietti, A. A. Natale, C. G. Roldao and R. Rosenfeld, Phys. Lett. B **497** (2001) 243 [arXiv:hep-ph/0009289].
- [43] R. M. Godbole, D. J. Miller and M. M. Muhlleitner, JHEP **0712**, 031 (2007) [arXiv:0708.0458 [hep-ph]].
- [44] T. Plehn, D. L. Rainwater and D. Zeppenfeld, Phys. Rev. Lett. **88**, 051801 (2002) [arXiv:hep-ph/0105325].
- [45] C. P. Buszello and P. Marquard, arXiv:hep-ph/0603209.
- [46] P. Niezurawski, A. F. Zarnecki and M. Krawczyk, Acta Phys. Polon. B **36**, 833 (2005) [arXiv:hep-ph/0410291].
- [47] E. A. Kuraev and V. S. Fadin, Sov. J. Nucl. Phys. **41**, 466 (1985) [Yad. Fiz. **41**, 733 (1985)].
- [48] M. Drees and R. M. Godbole, Z. Phys. C **59**, 591 (1993) [arXiv:hep-ph/9203219].
- [49] P. Chen, Phys. Rev. D **46**, 1186 (1992).
- [50] B. A. Kniehl, Nucl. Phys. B **352**, 1 (1991); Nucl. Phys. B **357**, 439 (1991)
- [51] M. C. Gonzalez-Garcia, Int. J. Mod. Phys. A **14**, 3121 (1999) [arXiv:hep-ph/9902321]; V. Barger *et al.*, Phys. Rev. D **67**, 115001 (2003) [arXiv:hep-ph/0301097].
- [52] J. F. Gunion, H. E. Haber and J. Wudka, Phys. Rev. D **43** (1991) 904.

- [53] A. Mendez and A. Pomarol, Phys. Lett. B **272**, 313 (1991).
- [54] D. Choudhury, A. Datta and K. Huitu, Nucl. Phys. B **673**, 385 (2003) [arXiv:hep-ph/0302141].
- [55] W. Buchmuller and D. Wyler, Nucl. Phys. B **268**, 621 (1986).
- [56] B. Grzadkowski and J. Wudka, Phys. Lett. B **364**, 49 (1995) [arXiv:hep-ph/9502415].
- [57] W. Kilian, M. Kramer and P. M. Zerwas, Phys. Lett. B **381**, 243 (1996) [arXiv:hep-ph/9603409].
- [58] K. Rao and S. D. Rindani, Phys. Lett. B **642**, 85 (2006) [arXiv:hep-ph/0605298]; Phys. Rev. D **77**, 015009 (2008) [arXiv:0709.2591 [hep-ph]]
- [59] A. Djouadi, J. Kalinowski and M. Spira, Comput. Phys. Commun. **108**, 56 (1998) [arXiv:hep-ph/9704448].
- [60] K. Hagiwara, A. D. Martin and D. Zeppenfeld, Phys. Lett. B **235**, 198 (1990).
- [61] D. P. Roy, Phys. Lett. B **277** (1992) 183.
- [62] B. K. Bullock, K. Hagiwara and A. D. Martin, Phys. Rev. Lett. **67** (1991) 3055.
- [63] B. K. Bullock, K. Hagiwara and A. D. Martin, Nucl. Phys. B **395** (1993) 499.
- [64] S. Raychaudhuri and D. P. Roy, Phys. Rev. D **52** (1995) 1556.
- [65] S. Raychaudhuri and D. P. Roy, Phys. Rev. D **53** (1996) 4902.
- [66] G. Bella, Nucl. Phys. Proc. Suppl. **40** (1995) 475.
- [67] M. Guchait and D. P. Roy, arXiv:0808.0438 [hep-ph].
- [68] M. M. Nojiri, Phys. Rev. **D51** (1995) 6281.
- [69] R. M. Godbole, M. Guchait and D. P. Roy, Phys. Lett. B **618**, 193 (2005) [arXiv:hep-ph/0411306].
- [70] S. S. Biswal, D. Choudhury, R. M. Godbole and Mamta, arXiv:0710.2735 [hep-ph].
- [71] A. Pilaftsis and C. E. M. Wagner, Nucl. Phys. **B553**, 3 (1999); M. Carena, H. E. Haber, H. E. Logan and S. Mrenna, Phys. Rev. D **65**, 055005 (2002).
- [72] D. Choudhury and Mamta, Phys. Rev. **D74** (2006) 115019 [arXiv:hep-ph/0608293]; Prana **mana** **69**, 795 (2007).
- [73] I. Sahin, Phys. Rev. D **77**, 115010 (2008) [arXiv:0802.0293 [hep-ph]].
- [74] R. W. Assmann *et al.*, SLAC-REPRINT-2000-096.
- [75] S. Dutta, K. Hagiwara, and Yu Matsumoto, arXiv:0808.0477v1 [hep-ph].